BACHELOR THESIS

A 100 year hydrographical record of the Barsnesfjord, Western Norway and its environmental application

by
Sabrina Kaufmann

Candidate number 104

Bachelor Thesis in Geology

GE491
28.05.2014

SOGN OG FJORDANE
UNIVERSITY COLLEGE

www.hisf.no

Agreement regarding the electronical deposit of scientific publications in HiSF Brage – Institutional archive of Sogn og Fjordane University College

The author hereby gives Sogn og Fjordane University College the right to make this thesis available in HiSF Brage provided that the thesis is awarded gr*ade B* or better.

I guarantee that I - together with possible co-authors - have the right of authorship to the material thus have legal rights to allow HiSF to publish the material in Brage.

I guarantee that I have no knowledge or suspicion indicating that this material is illegal according to Norwegian law.

Please fill in your candidate number and name below and tick off the appropriate answer:

Sabrina Kaufmann

Candidate number 104

YES __   NO__

List of Contents

Glossary

Azores High	High air pressure system located in the North Atlantic forming over the Azores islands.
Brackish water	Salty water, which is not as salty as sea water. The salinity lies between 0.5 to 30‰
Basin water	The deep water layers of a fjord below the sill. It is often stagnant, but is renewed with coastal water occasionally due to inflows of oxygen rich water.
Coriolis Force	As a result of the earth's rotation, moving objects are deflected to the right in the northern hemisphere and to the left in the southern hemisphere.
Downwelling	The movement of surface water to deeper depths
Estuarine Circulation	The result of the freshwater runoff. It is driven by the density differences between the brackish water layer in a fjord and the coastal water
Great Salinity Anomaly (GSA)	An event lasting from 1969 to 1982 where the upper layers of the Nordic Seas experience a reduction in salinity.
Gulf Stream	A warm ocean surface water current, starting in the Caribbean Sea and crossing the North Atlantic ocean.
Icelandic Low	Low air pressure system forming over Iceland.

Glossary

Mid-ocean ridge	An underwater mountain range which was formed by plate tectonic processes and consists of spreading areas.
Nordic Seas	The collective name of the ocean areas of the Greenland Sea, the Iceland Sea and the Norwegian Sea.
Norwegian Coastal Current (NCC)	Also known as the Norwegian Current, it is a water current that flows northward along the Norwegian coast.
Sill	A ridge at a shallow water depth, which is separating the basin water of a fjord from the next water body.
Station Mike	Ocean Weather Ship Station Mike is located in the Norwegian Sea at 66°N latitude and 2°E longitude. It has measured oceanographic parameters down to 2000m water depth on a daily basis from 1948 to 2009.
Thermohaline Circulation (THC)	A density-driven circulation in the ocean caused by differences in temperature and salinity between the ocean surface water, intermediate water, and deep water.
Upwelling	The movement of cold, deep, often nutrient-rich water to the surface mixed layer
Westerlies	Prevailing winds between 30 and 60 degrees latitude, blowing from the high pressure area towards the poles

Abstract

A 100 year hydrographical data set of the parameters temperature, oxygen and salinity is analyzed from the water column of the Outer Barsnesfjord, Western Norway, at intervals from 0 m to 75 m water depth. After 1960, average water temperatures started to increase from approximately 6°C to 8°C in the basin waters of the fjord. Beginning at the same time, oxygen and salinity concentrations were decreasing in the Barsnesfjord basin waters: oxygen from 6-4 mg/l to 4-1.5 mg/l and salinity from 33.5‰ to 32.5‰. Similar changes of increasing temperature and decreasing oxygen and salinity occurred also in the intermediate water layer and the surface water layer of the Barsnesfjord although less pronounced. These hydrographical variations are attributed to simultaneous changes observed in the hydrography of the Nordic Seas, as well as to changes in the NAO (North Atlantic Oscillation) winter index. It is concluded that hydrographical changes in the Barsnesfjord are highly susceptible to the open ocean hydrography of the Nordic Seas. In addition, the upper water layers might partly be influenced by changes in freshwater input due to damming of rivers in the region since the middle 1970s.

Acknowledgment

1. Introduction

With a unique 100 year record of measurements of the parameters oxygen, temperature and salinity in the Barsnesfjord, Western Norway, changes in the water body can be observed. These changes are namely an increase in temperature and a decrease in oxygen concentration and salinity. This bachelor thesis focuses on the question what caused these changes. Considering this, the measurements of the Barsnesfjord will be compared with those from the Sogndalsfjord (Surlemont 2012; Dale *et al. in preparation*) and those of the Nordic Seas, which have been taken at the "Ocean Weather Ship Station Mike" (Dickson & Østerhus 2007). Since the North Atlantic Oscillation (NAO) is the leading pattern of weather and climate variability over the Northern Hemisphere (Hurrell 1995; Hurrell *et al.* 2003; Hurrell & Deser 2009), the NAO also will be analyzed and compared with the changes depicted in the Barsnesfjord.

1.1 Fjords

The following information about fjords is taken from the books "*Fjords: Processes and Products*" (Syvitski *et al.*, 1987) and "The Norwegian Coastal Current-Oceanography and Climate" (Sætre, 2007).

Norwegian fjords are estuaries formed by glacial over-deepening of river valleys throughout the Quaternary time period, i.e. the past 2 million years. In total 23 phases of major ice advance (ice ages) and ice retreat (interglacials) have culminated in the last glacial maximum, around 18.000 years before present (B.P.), forming the fjords as a product of ice and sea-level fluctuation. The sediments in these overdeepend coastal basins have accumulated since around 15.000 to 10.000 B.P. (Aa, 1982), consisting of glacial and proglacial deposits of the last deglaciation, and of Holocene sediment infill of the last 10.000 years. Many fjords have a sill in the mouth area and one or more basins. All silled fjords are immature estuaries and therefore sites of sediment accumulation. Fjords are transition regions between land and the open ocean.

Therefore they are regions of strong physical and chemical gradients, where fresh water and salt water mix and react. Fjords are the main source of freshwater to the Norwegian Coastal Current with an annual freshwater runoff from Norway of approximately 400 km^3/year. The runoff shows a clear seasonal signal, with a maximum from May to June and a minimum from February to March. There exists a strong correlation between the NAO winter index and the annual precipitation in Western Norway. A high NAO winter index means strong westerly winds over Northern Europe and thus increased precipitation. The freshwater in the fjords is forced out towards the coast, following a pressure gradient, while flowing in a brackish upper layer. Winds, friction and tides mix the freshwater with the more saline water beneath. When the freshwater finally reaches the coast, it is well mixed, with a slightly lower salinity than the coastal water masses.

The typical arrangement found in fjords that have a sill is that of a three layered water body (Figure 1). The upper layer is a fresh surface layer, followed by an intermediate layer, which is located between the surface layer and the sill depth, and a deep layer, which can be found below the intermediate layer. The fresh upper layer contains melt water from the glacier and terrestrial runoff, for example snowmelt, river run-off, and precipitation. Surface waters hold a wide range of salinities, oxygen, and temperatures, which is primarily due to surface warming, variability in discharges and the phytoplankton production. In the surface layer the fresh water is transported from the fjord to the coast. The intermediate water masses are often strongly altered from their original characteristics due to mixing with the fresh surface water and the saline deep waters (F. R. Cottier, 2010). The flow in the intermediate layer is triggered by differences in the pressure and density between the coast and the fjord. Variations in wind directions along the coast are partly responsible for the density differences inside and outside a fjord. The intermediate water transport is considered to be greater than in the surface layer. The deep layer contains the basin water, which can be stagnant, but is renewed with coastal water occasionally.
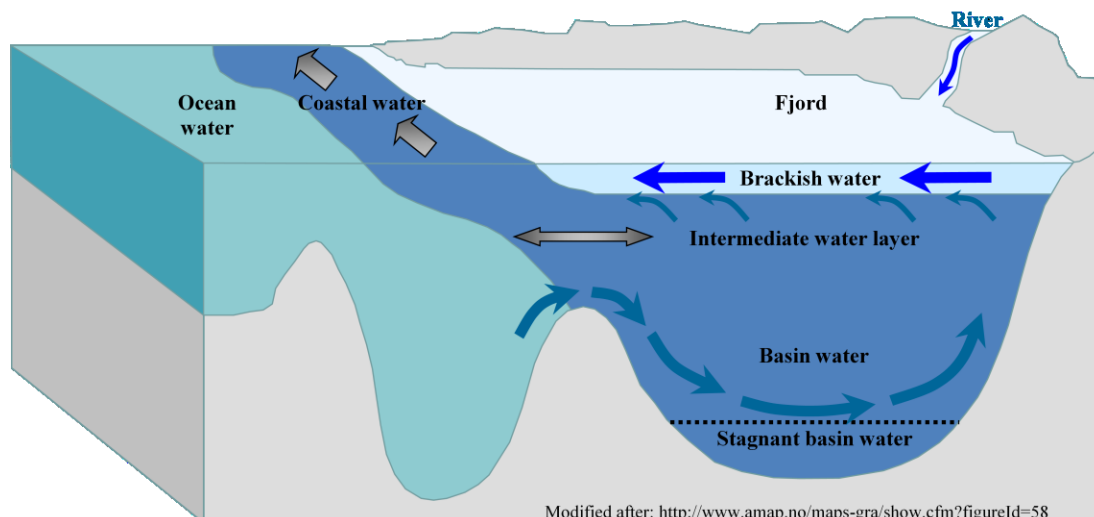
Figure 1: Water layers and circulation pattern in a fjord. The process of water exchange due to estuarine circulation is illustrated by the light blue arrows (water inflow) and dark blue arrows (water outflow). Figure used from Keith Surlemont

1.2 Exchange Processes in Fjords

There are different water exchange processes in fjords. One of them is the freshwater-induced exchange, which is called estuarine circulation and occurs in the upper layer of the fjord. It is the result of the freshwater runoff and is driven by the denisty differences between the brackish water layer in a fjord and the coastal water (Sætre, 2007). The seaward flowing brackish water is continously mixed with seawater. Closing the esturine circulation cycle, there is an inflow of coastal water beneath this outflowing surface brackish water to compensate the salt water transport by the brackish water flow. Compared to other exchange components, this freshwater- driven coast/ fjord water exchange is small. Another water exchange component in fjords is the locally wind-driven exchange. Wind stress that is imposed on the surface water of a fjord forces the water to move in the direction of the wind and slightly to the right. This wind-driven flow gets rapidly smaller the deeper it gets, at a depth of around 10-20 meter no sign of this wind-driven flow can be found. That means that this exchange process is most important for the mixing of the surface brackish layer inside the fjord, whereas its contribution to the mixing of coastal and fjord water is insignificant. A significant mixing may also occure where a river enters the brackish layer of a fjord (Stig Skreslet, 1986). An important exchange factor for coastal and fjord water is the exchange driven by sea-level differences.

The sea level varies due to tides and meterological forces like wind and atmospheric pressure. The greatest influence on the coast/fjord water exhcange is governed by semidiurnal tides due to their large tidal differences and their rapid fluctuations. Another exchange of coastal water and fjord water is driven by horizontal density differences which are generated by density fluctuations in the coastal water. This density distribution of the coastal waters can be changed by advection of new water masses of different properties as well as wind-induced coastal upwelling or downwelling. The intermediate water of the fjords is flushed into the open ocean during upwelling events. During downwelling events the density of the water at the sill depth of the fjord increases, which makes a renewal of the deep water more likely. The renewal of the basin water is an important mechanism for silled fjords. If the water outside the sill is denser then the water of the fjord basin, it can be lifted over the sill (Perillo, 1995). During this inflow, a density current develops and replaces the basin water inside the fjord. These renewal events can be triggered by tides, weather systems like land and sea breeze or atmospheric pressure as well as by seasonal events like monsoonal winds and runoff variations. The heavy "renewing" water, which enters the fjord over the sill, sinks down to the botton of the basin, due to gravity and density contrasts. The oxygen conditions in a fjord depend on periodical water renewals as well as on the supply of organic matter. In shallow silled fjords that also have a long residence time the basin water can turn anoxic. With none or extremely low oxygen concentrations over a long time period, benthic biota is not able to survive and the fauna within the fjord basins can become extinct due to periods with anoxic conditions.

1.3 The Barsnesfjord
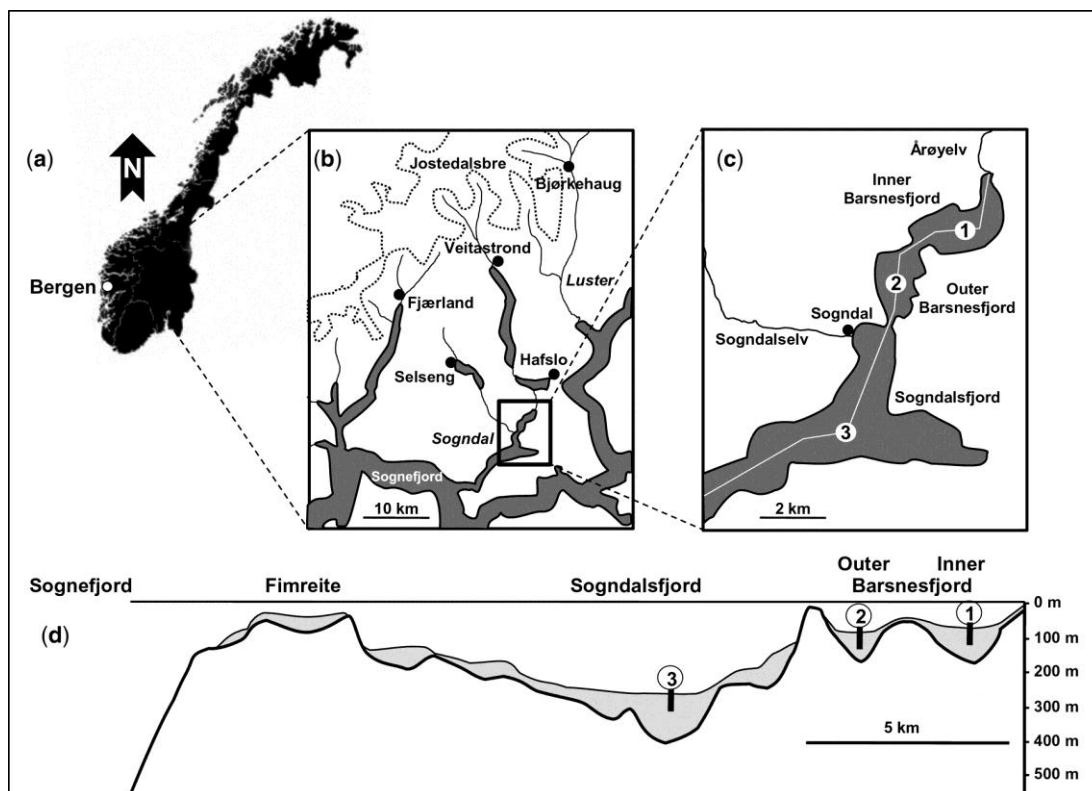
Figure 2: Regional map of the Sogndalsfjord area: (a) Map of Norway (b) Extract of the Sognefjord (c) Map of the Sogndalsfjord (d) cross-section showing the bathymetry of the Sogndalsfjord (Paetzel & Dale, 2010).

The Sogndalsfjord and the Barsnesfjord are tributaries of the Sognefjord, Western Norway (Figure 2). The Barsnesfjord consists of an inner basin, which is periodically anoxic and has a maximum water depth of 66 m, and of an outer basin, which is mostly oxic and has a maximum water depth of 80 m (Paetzel & Dale, 2010). The Inner and the Outer Barsnesfjord are connected by a 29 m deep sill. The Sogndalsfjord, which has an oxic basin of the maximum depth of 260 m, is connected with the Outer Barsnesfjord by a 7.5 m deep sill (Figure 2c). At Fimreite, the Sogndalsfjord connects to the >900 m deep Sognefjord with a 25 m deep sill. Due to these shallow sills, the water circulation in the Barsnesfjord is restricted. The major freshwater inflow comes from the river Årøyelv (Figure 2c), which is located at the northern end of the Inner Barsnesfjord basin. The Årøyelv is connected with the lake Hafslovatnet, which lies southwest of Hafslo (Figure 2b). Across a shallow sill, the lake Hafslovatnet is connected with the lake Veitastrondvatnet, which lies south of Veitastrond (Figure 2b).

Both lakes receive their freshwater from a catchment area of 429 km², which also includs the glacial river inflow from the glacier Jostedalsbre, which is located in the north. Due to the fluvial freshwater input, the water column of the Inner Barsnesfjord is strongly stratified from approximately April to September, with an almost fresh surface layer (ca. 2-4 m deep) and a halocline going down to ca. 15 m (Figure 3). The oxygen concentrations in the fjord bottom water decrease over time due to the rare water renewal. This leads to anoxic periods in the Inner Barsnesfjord. There are also similar seasonal water stratifications in the Outer Barsnesfjord. Even though the water circulation is stronger in the Outer Barsnesfjord, which causes periodically oxic conditions in bottom waters and sediment, the oxygen levels fall at times below the critical value of 2 mg/l.
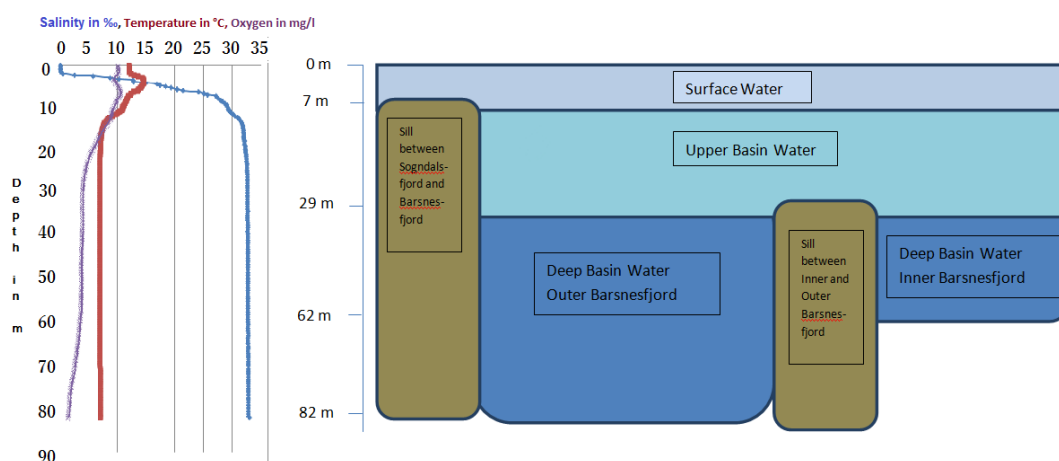
Figure 3: Drawing of the Inner and Outer Barsnesfjord with their sills and depth profiles. The graph on the left shows the values of the Outer Barsnesfjord from the 3.September 2013, namely Salinity in ‰, Temperature in °C, Oxygen in mg/l. Drawing of the Barsnesfjord by Sabrina Kaufmann, 2014. Graph modulated by Sabrina Kaufmann with Data from Torbjørn Dale, 2013.

Figure 3 shows a drawing of the Inner and Outer Barsnesfjord, visualizing the sills that separate the Sogndalsfjord and the Barsnesfjord with a sill depth of approximately 7.5 m and the sill that separates the Outer and the Inner Barsnesfjord with a sill depth of 29 m. Their depth profiles can also be seen. For the Outer Barsnesfjord the surface water layer lays within the first 8 m, the upper basin water lays between 8 and approximately 30 m and the deep basin water lies between 30 m down to 82 m. The surface water layer and the upper basin water layer of the Inner and Outer Barsnesfjord are connected, whereas the deep basin waters of the Inner and Outer Barsnesfjord are two separate water bodies.

A water renewal happens only with an inflow from the Outer Barsnesfjord into the Inner Barsnesfjord, bringing initially poor low-oxygen water from uplifted old basin water from the Outer Barsnesfjord into the Inner Barsnesfjord. The graph on the left shows values of the Outer Barsnesfjord from the year 2013, namely Salinity in ‰, Temperature in °C and Oxygen in mg/l. It can be compared with the drawing to visualize the different values of the parameter in various depths.

1.4 The Nordic Seas
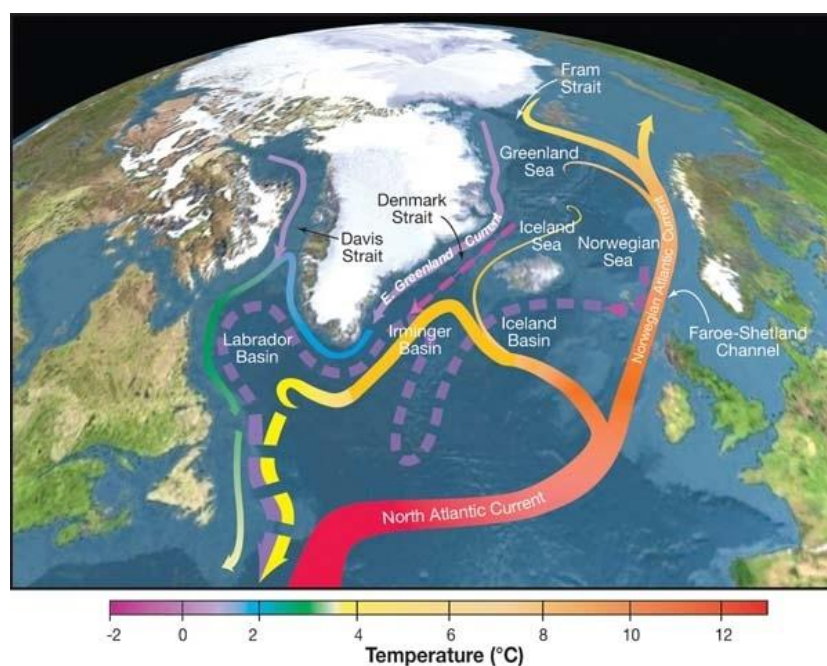
Figure 4: Topographic map of the Nordic Seas and subpolar basins with schematic circulation of surface currents (solid curves) and deep currents (dashed curves) that form a portion of the Atlantic meridional overturning circulation. Colours of curves indicate approximate temperatures. Source: R. Curry, Woods Hole Oceanographic Institution/Science/USGCRP, 2014

The Nordic Seas are divided into the Greenland, Iceland and Norwegian Seas because of their topographic features (Figure 4). One of these features is the mid-ocean ridge, with the three main parts known as the Kolbeinsey Ridge, the Mohn Ridge and the Knipovich Ridge, as can be seen in Figure 5. The Kolbeinsey Ridge extends from the North Icelandic shelf to the latitude of Jan Mayen, where it is broken by the Jan Mayen Fracture Zone. The Mohn Ridge has a complex topography and is characterized by many isolated elevations.

It has depths ranging between 1000 and 2000 m. The Knipocich Ridge stretches from the Mohn Ridge to the Fram Strait and has its shallower crests at about 1000 m depth.
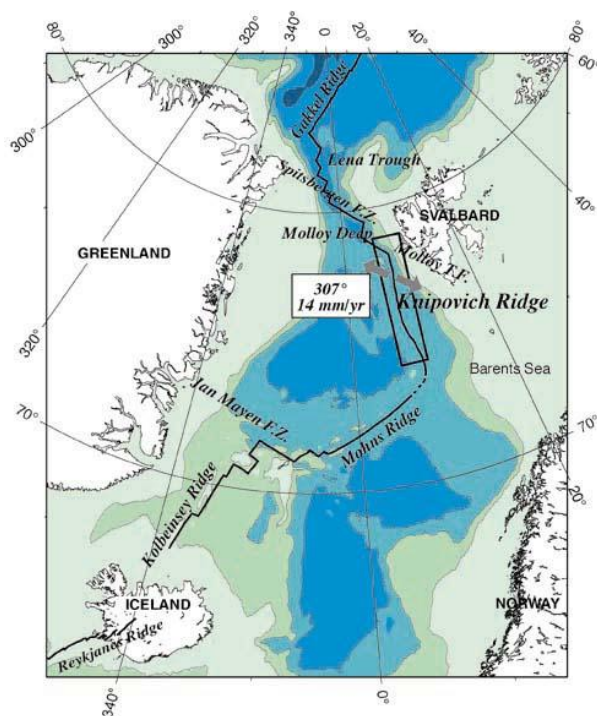
Figure 5: Kolbeinsey Ridge, the Mohn Ridge and the Knipovich Ridge

There are four major basins in the Nordic Seas (Figure 6) which are divided due to the bathymetry (Blindheim & Østerhus, 2005). There are two deep basins in the Greenland Sea west of the Mid-ocean Ridge. The Greenland Basin, with depths from 3400-3600 m is the larger and deeper one. Separated by the Greenland Fracture Zone, is the smaller and shallower Boreas Basin with depths around 3200 m. In the Iceland Sea, south of the Jan Mayen Fracture Zone, the Iceland Plateau can be found. It is located in the area between Iceland and Jan Mayen to the east of the Kolbeinsey Ridge. The Norwegian Sea has two deep basins, the Norwegian and the Lofoten Basin. The Norwegian Basin is the largest and deepest basin in the Nordic Seas with depths mainly between 3200-3600 m, but also has a narrow trough with depths reaching down to 3800 m. The Norwegian Basin extends northward from the Iceland-Faroe Ridge and eastward from the Iceland Plateau to the Vøring Plateau and the continental slope of the Norwegian coast.

The Lofoten Basin is smaller and shallower, around 3200 m deep, and lies north of the Norwegian Basin and the Vøring Plateau. Between Spitzbergen and Greenland lays the Fram Strait which connects the Nordic Seas with the Arctic Ocean. The Fram Strait has a sill depth of around 2600 m. The Greenland-Scotland Ridge forms the border towards the North Atlantic to the south. The deepest sills here are located in the Faroe Bank Channel with around 850 m sill depth and in the Denmark Strait with around 620 m.
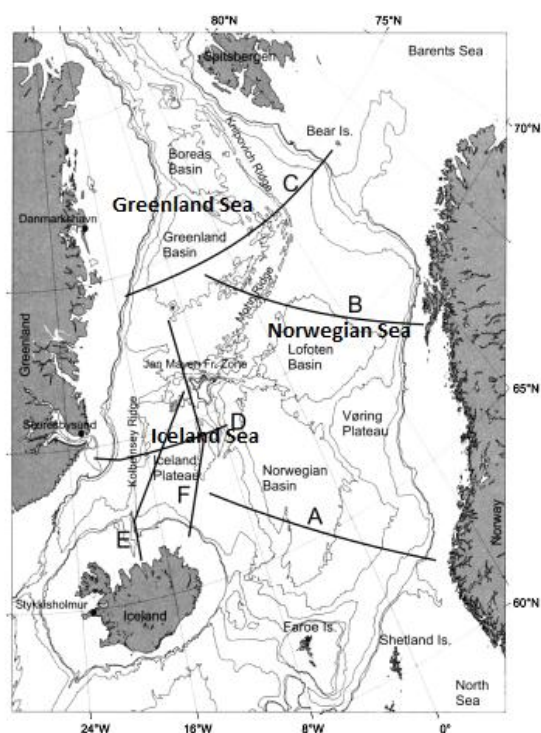

Figure 6: The Nordic Seas Bathymetry (Blindheim and Østerhus, 2005). Notice: Greenland Sea, Norwegian Sea and Iceland Sea are edited into the original picture.

1.5 The vertical structure of the ocean
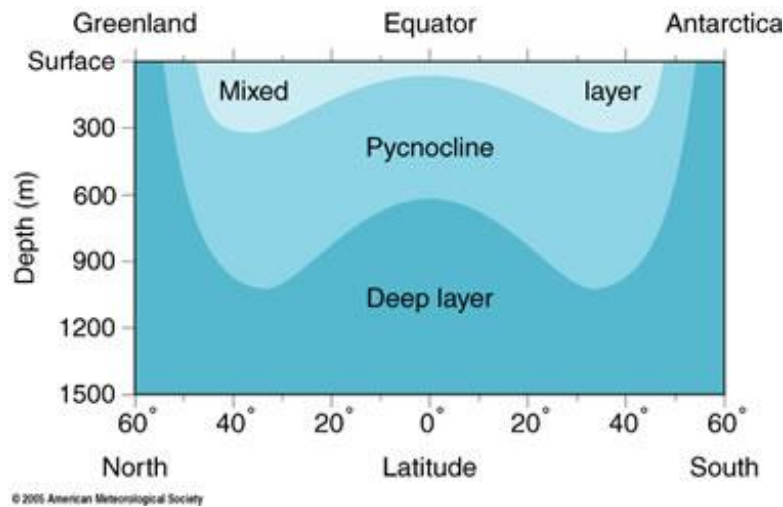
Figure 7: A cross-sectional longitudinal profile of the Atlantic Ocean from 60 degrees N to 60 degrees S showing the location of the mixed layer, pycnocline, and deep layer. Note that the ocean (and deep layer) extends to depths of 4000 to 6000 m.

The ocean is divided into three horizontal depth zones based on density (Figure 7): the mixed surface layer, pycnocline, and deep layer (American Meteorological Society, 2006). Only at high latitudes, the pycnocline and mixed layer are absent.

Wind-driven surface currents occur mainly at the ocean's uppermost 100 m and depend on the depth of the pycnocline. This is due to the thickness of the surface mixed layer, which is usually 100 m or less. Through the pycnocline little kinetic energy is able to penetrate into deep water, since it acts as a porous boundary. The strongest currents occur in the ocean's surface layer, although some surface currents, like the Gulf Stream, can be relatively strong to depths of several hundred meters. Surface currents change often, since they respond to variations in wind, precipitation, heating or cooling. A mixing of the surface waters by the wind produces a well-mixed layer of uniform or almost uniform density. Because of that, the ocean surface is called the mixed layer. The pycnocline separates the mixed layer from the deep layer and thus hinders a vertical transport within parts of the ocean.

 In the pycnocline the water density increases rapidly with depth due to changes in temperature and salinity. The pycnocline is a thermocline and a halocline. A decline in temperature with depth is responsible for the increase in density, which makes the pycnocline a thermocline**.** The increase in salinity on is responsible for the increase in density with depth, which makes the pycnocline a halocline**.** The pycnocline extends typically to a depth of 500 to 1000 m. The dark, cold deepwater below the pycnocline accounts for most of the oceans volume. Within the deep layer, density increases gradually with depth and water moves slowly. Because of that there are only few places where the water moves fast enough to be considered a current. These deep currents usually occur near the bottom of the ocean.

1.6 Circulation in the upper layers in the Nordic Seas

The topographical steering and the prevailing wind forcing characterize the surface currents within the Nordic Seas and influences water-mass structure and formation (Blindheim & Rey, 2004). The schematics of the main circulation features in the upper layers are shown in Figure 8. The western area is dominated by the East Greenland Current with its major branches, the Jan Mayen Current and the East Icelandic Current. Being blocked by the Jan Mayen Fracture Zone, the Jan Mayen Current flows into a cyclonic gyre in the Greenland Basin. The East Icelandic Current flows along the North Icelandic slope into the southwestern Norwegian Basin. It forms the Arctic Front over the northern slope of the Iceland-Faroe Ridge, known as the Iceland-Faroe Front, as it mixes with the Atlantic Waters of the Faroe Current. In the south-eastern Nordic Seas, the upper layers have the warmest and saltiest water of the region due to the inflow of the Norwegian Atlantic Current through the Faroe-Shetland Channel, as well as across the Iceland-Faroe Ridge (Skjoldal, 2004). The Norwegian Atlantic Current is considered to be a continuation of the Gulf Stream which influences the climate in Norway and northern Europe by heat transfer (Global Britannica, 2014). To the north, much of the Atlantic Water of the West Spitsbergen Current re-circulates into the Fram Strait. In the East Greenland Current it mixes with waters returning from the Arctic Ocean and forms the Re-circulating Atlantic Water, which appears as intermediate water masses.
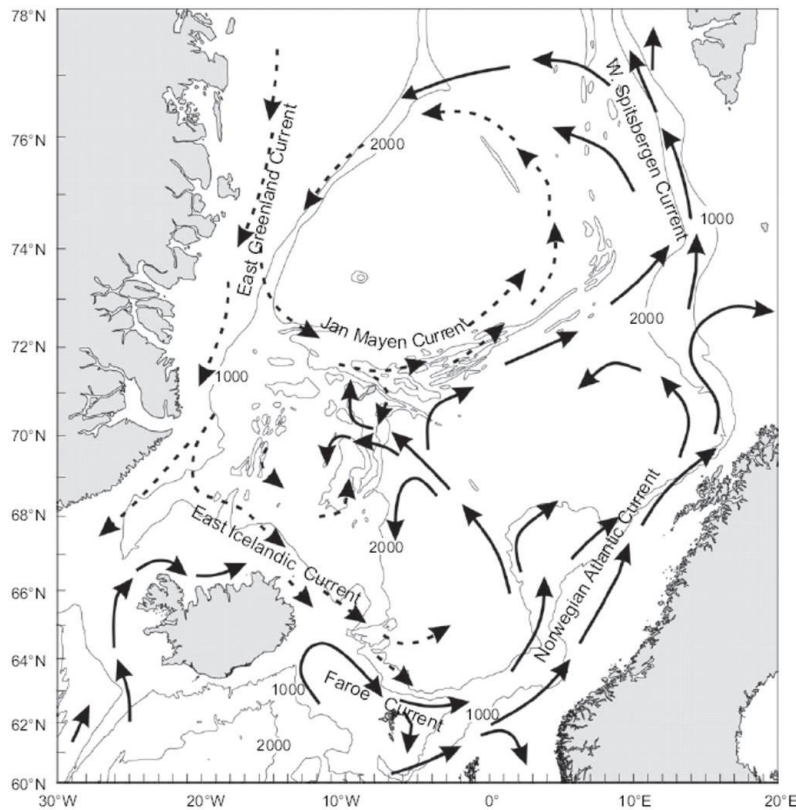
Figure 8: Schematic illustration of the current system in the Nordic Seas. Arrows with broken lines represent Arctic waters. Solid lines represent Atlantic Water (Blindheim & Rey, 2004).

1.7 Deep water circulation

While winds drive ocean currents in the upper 100 meters of the ocean's surface, there are also deep-ocean currents that flow thousands of meters below the surface. These currents are driven by differences in the density of the ocean water, depending on temperature (thermo) and salinity (haline). Because of that, this process is known as thermohaline circulation (NOAA Ocean Service Education, 2014). In the Polar Regions, ocean water gets very cold when heat is emitted to the air and sea ice forms. The surrounding seawater gets saltier due to this sea ice formation. Since the salt does not freeze, the salt is left behind in the ocean water. When the water gets saltier, its density increases at the same time and it starts to sink down. This sinking water needs to be replaced, therefore surface water is drawn in to replace the sinking water, which eventually becomes cold and salty and also starts to sink down. This sets the deep-ocean currents in motion and drives the global conveyer belt.
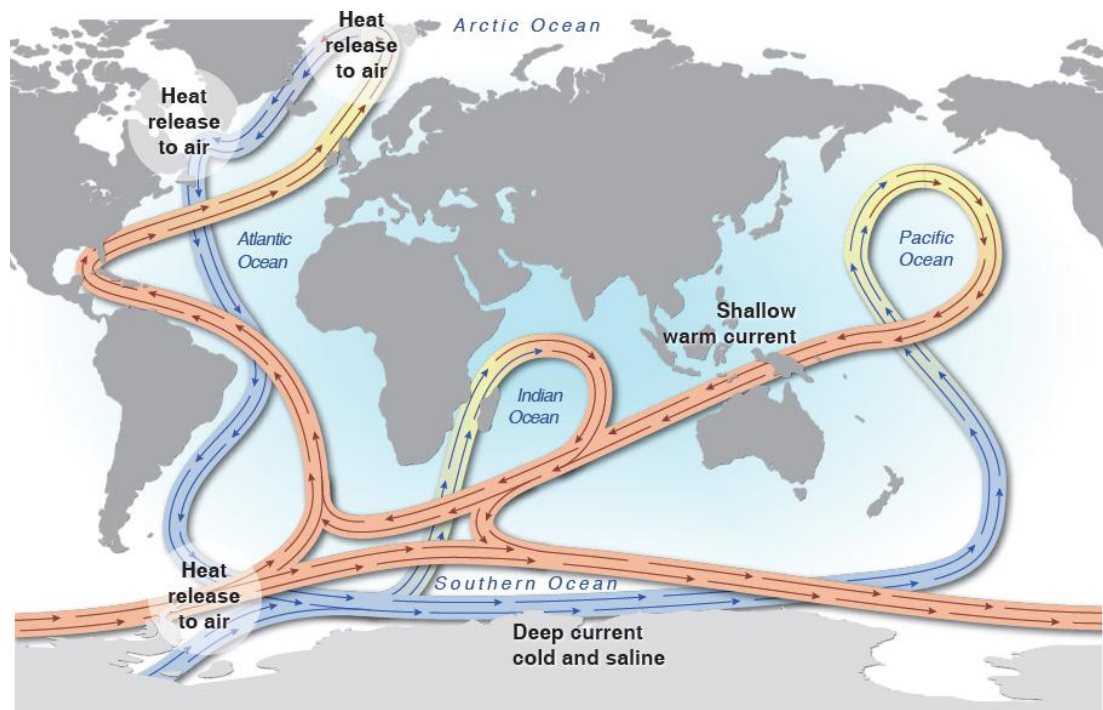
Figure 9: Schematic figure showing the three main areas where deep water is formed: in the Labrador Sea, in the Nordic Seas, and in the Antarctic Weddel Sea. Deep water is formed when water cools and sinks, thereby releasing heat to the air. After sinking, the water circulates around the world ocean, eventually rising up in the Indian and North Pacific oceans. (UNEP/GRID-Arendal, 2007)

The conveyor belt begins at the oceans surface near the North Pole in the North Atlantic, with heavy water sinking down to the bottom to form deep water (Figure 9). The deep water then moves south between the South America and Africa toward Antarctica. Here is also another site of sinking of surface water, which is even denser than the deep water of the North Pole and thus sinks below it (Torbjørn Dale, 2014, *personal* communication). The main deep water current then splits into two sections, with one section moving to the Indian Ocean and the other to the Pacific Ocean. As these two sections travel northward toward the equator, they warm up and become less dense. This causes them to rise to the surface. They loop back southward and westward to the South Atlantic and eventually return to the North Atlantic, where the cycle starts again.

1.8 NAO-Index

The following information about the NAO is taken from Visbeck (2014) and Sætre (2007). Since there are energy exchanges between ocean and atmosphere, the ocean reflects the climatic fluctuations in the atmosphere. In the North Atlantic, the North Atlantic Oscillation, short NAO, is the most dominant climatic feature.

The NAO is a large scale seesaw in atmospheric mass between the subtropical high air pressure in the Azores and the polar low in Iceland. Monthly pressure differences between the Azores High and the Iceland Low express the NAO index, which varies from year to year and thus have a distinct influences on physical and biological conditions in the Nordic Seas. These influences can be determined best during the winter months, when the intensity of the atmospheric activity is the highest.
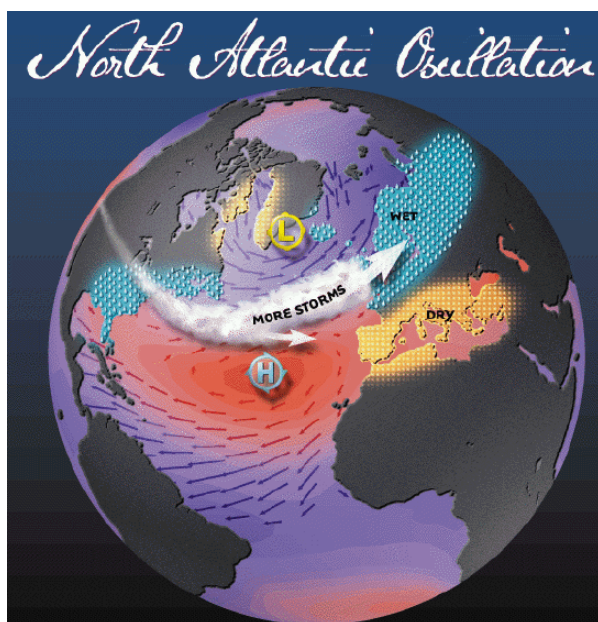
Figure 10: Schematic view of the North Atlantic Oscillation (NAO winter index). The sketch indicates a positive NAO winter index, leading to wet and mild winters in Northern Europe (Visbeck, 2014).

The positive NAO index phase shows a stronger than usual subtropical high pressure centre and a deeper than normal Icelandic low (Figure 10). This strong air pressure difference between the Azores High and the Iceland Low drives south-westerly winds, resulting in more and stronger winter storms crossing the Atlantic Ocean on a more northerly track. This leads to warm and wet winters in north-western Europe and to cold and dry winters in Mediterranean region.

Figure 11: Schematic view of the North Atlantic Oscillation (NAO winter index). The sketch indicates a negative NAO winter index, leading to dry and cold winters in Northern Europe (Visbeck, 2014).

The negative NAO index phase shows a weak subtropical high and a weak Icelandic low (Figure 11). The pressure gradient is reduced, which results in fewer and weaker winter storms, which cross on a direction from west to east and lead to wetter conditions in the Mediterranean. Northern Europe receives cold and dry air, which implicates that there is less precipitation in Northern Europe than under a positive NAO index.

1.9 Environmental impact of oxygen concentrations
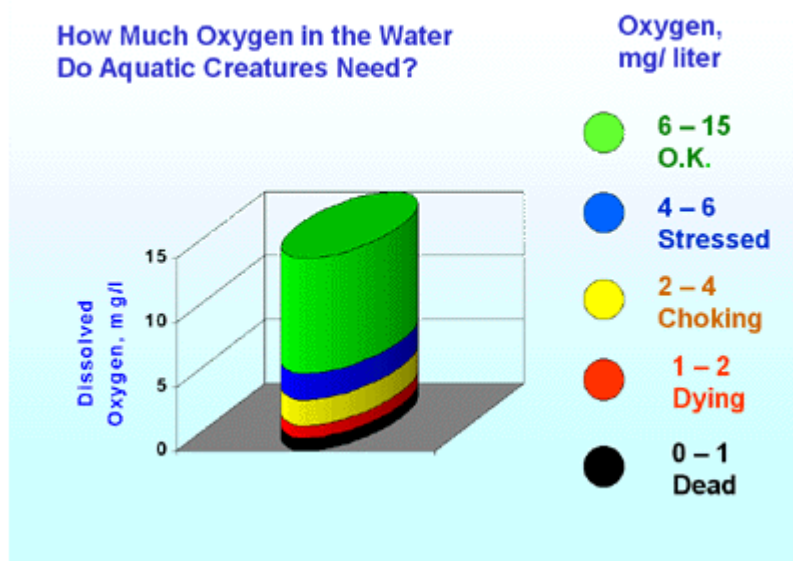
Figure 12: Critical oxygen concentrations for freshwater organisms (EPA, 2012)

Oxygen is an important element to all forms of life. Oxygen dissolves from air into the surface of the water body by diffusion and is also produced by the phytoplankton and plants in the water body by photosynthesis. Good living conditions for aquatic organisms occur with oxygen concentrations between 6 and 12 mg/l (Figure 12). If dissolved oxygen levels in water drop below 5 mg/l, aquatic life is put under stress. The lower the concentrations get, the greater the stress for the organisms. With oxygen concentrations between 2 and 4 mg/l many organisms get into choking conditions. The critical oxygen concentration is reached at 2 mg/l (EPA, 2012). Many organisms start dying at concentrations between 1 and 2 mg/l. Below 1 mg/l most eukaryotic aquatic life is not possible, apart from a very small range of organisms and bacteria that are adapted to anoxic water conditions.

2. Objectives

1) How did the parameters temperature, oxygen concentration and salinity vary over the last 100 years in the Barsnesfjord?

2) Are these variations within the Barsnesfjord and the Sogndalsfjord related to the variations at the Nordic Seas?

3) Are there overall environmental change mechanisms (e.g. the NAO-Index) that could explain the observed variations in the water masses?

3. Methods

The hydrographical samples were taken from two regions:

1) The Nordic Seas

Measurements of oxygen, temperature and salinity are taken from the ocean weather ship "Station Mike". The data was downloaded from the Eurosites webpage http://www.eurosites.info/stationm.php . The location of Station M is 66°N 2°E and the CTD-sensor "Seabird 16-plus" was used. The measuring period is from 1948-2011.

2) The Barsnesfjord, Western Norway

Oxygen, temperature and salinity were taken over a long period from 1916-2013. For the fjord sampling from 1916-1956 a Nansen-Bottle was used and from 2001 on till 2013 a CTD-sensor. The location of the Barsnesfjord sampling is 61°13´N 07°05´E.

Table 1: Sampling devices and methods for the measurements in salinity, temperature and oxygen in the different periods.

Periods	Sampling device	Salinity	Temperature	Oxygen
1916-1956	Nansen	Titration	Reverse Thermometer	Winkler
1978	Nansen (?)	Titration (?)	Reverse Thermometer (?)	Winkler (?)
1984-1985	Nansen (?)	Salinoterm MC 5	Salinoterm MC 5	YSI-57 O_2-Meter
1991-1993	Rutner	Densimeter	Simple Thermometer	Winkler
2001-2013	CTD- SAIV SD204	CTD- SAIV SD204	CTD- SAIV SD204	CTD- SAIV SD204

Table 1 shows the different sampling devices that were used to measure the values of oxygen, temperature and salinity in the Barsnesfjord. In the first period from 1916-1956 the Nansen Bottle was used to take the water samples. From 1984/1985 the Nansen Bottle was most probably used as well to collect the water samples, only the methods to determine salinity, temperature and oxygen were different. It is very likely, that the values from 1984/1985 are too inaccurate to be included and were therefore left out. The values of all the parameter can still be found in Appendix B. For the year 1978 it is unsure which sampling device and which methods were used. Since the sampling was performed by the University of Bergen, as in the years from 1916-1956, the sampling device and methods were most probably the same. The sampling device from the period of 1991-1993 is the Rutner Water Sampler. The methods used to determine temperature and oxygen were the same as in the first period from 1916-1956. Only salinity was determined differently, namely with a densimeter, which is not as accurate as the titration method. The sampling device of the last period from 2001-2013 was the CTD SAIV SD-204, which is a high quality CTD- sensor. The data collected with the CTD is therefore quite reliable and accurate.

3.1 Hydrographical measurements in the Nordic Seas

For the measurements in the Nordic Seas at "Station Mike" a CTD-sensor is used (Figure 13). In appendix A the mooring set up of the CTD station is shown. From different water depths between 50 and 2000m the Seabird 16-plus CTD-sensors measure the parameter temperature, oxygen concentration, salinity and density. The ocean weather station M was started in 1948 by the Norwegian Meteorological Institute (DNMI) and the University of Bergen. Until June 2009 Station Mike was operated as a manned weather ship called the Polar Front. In February 2010 a sub-surface mooring was deployed funded by Research Council of Norway. With Station M being located at the eastern margin of the Norwegian Sea deep basin, where a branch of the Atlantic current is entering the area, the location is chosen wisely for studying the Atlantic inflow and the Norwegian Sea Deep Water.
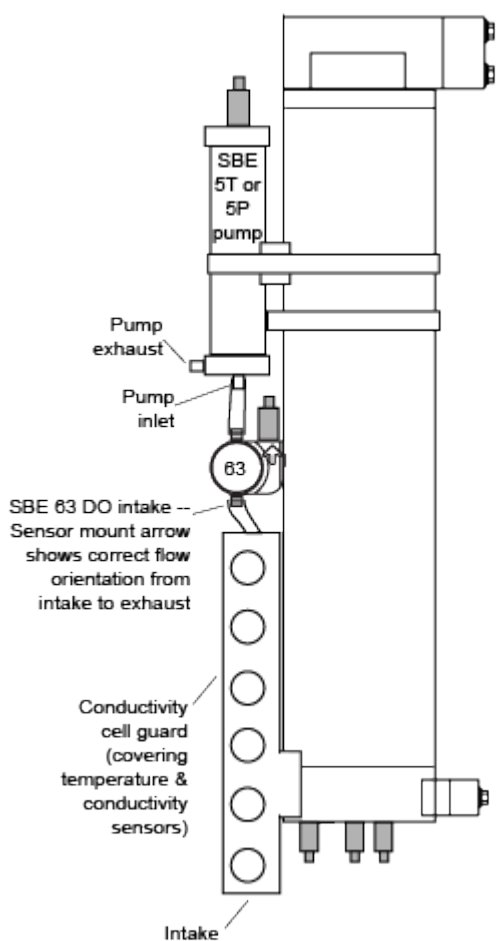

Figure 13: Seabird 16 plus CTD-sensor (seabird.com, 2014)

3.2 Hydrographical measurements in the Barsnesfjord

In 1916 the University of Bergen started to measure hydrographical parameters in the Barsnesfjord, namely temperature, salinity and oxygen. The fjord sampling can be divided into three time periods:

(1) University of Bergen, one to seven measurements per year between 1916 and 1956 and in 1978

(2) Sogn og Fjordane University College, one to eight measurements per year over three shorter time periods (1984-1985; 1991-1993)

(3) Sogn og Fjordane University College, one series of measurements every fall between 2001 and 2013

3.2.1 Measurements retrieved by a Nansen Bottle

In the first and second period of sampling, which were performed by the University of Bergen from 1916-1956 and in 1978 a Nansen Bottle was used (Figure 14). The sampling depths were 0, 5, 10, 20, 30, 40, 50, 60 and 75 meter. To be able to measure oxygen and salinity trough out a water body, water samples from various depths are needed. Fritjof Nansen developed in 1910 a water bottle that is able to collect a sample from a certain depth (Helmond, 2000). The Nansen Bottle consists of a metal cylinder with two interconnected rotating closing mechanisms at both ends. The bottle that is attached to a wire is lowered to the desired depth with both ends open so the water can flow through the Nansen bottle. A messenger is dropped down to trigger the turning mechanism, the bottle is turned upside down and the water is trapped. A new messenger is released from the now closed bottle and travels down to the next Nansen Bottle that will take a water sample at this depth. This process continues until the last bottle is closed. For measuring the temperature at a certain depth, a reversing thermometer was attached to the Nansen Bottle in a fixed frame (Department of Oceanography, 2005). When the bottle turns the reversing thermometer also turns, disconnects the mercury in the capillars from the bulb and thus "saves" the measured temperature at the sampling depth (Torbjørn Dale, 2014, *personal* communication).

The water samples of the Nansen Bottles were analysed using the Winkler titration method (Winkler, 1888) for the determination of the oxygen concentration, and the Mohr-Knudsen (Mohr, 1856) titration methods for salinity determination (Torbjørn Dale & Matthias Paetzel, 2011, personal communication).

Before turning   While it turns   After turning

Figure 14: Trapping water with the Nansen Bottle (Nichols & Williams, 2008).

3.2.2 Direct hydrographical measurements using a CTD-sensor

Since 2001 the Sogn og Fjordane University College has been taking yearly CTD measurements every fall as a part of the "From Mountain To Fjord"-program. These measurements were performed with CTD/STD – model SAIV SD204 (Figure 15). The SD204 measures, calculates and records sea water conductivity, salinity, temperature, depth (pressure), sound velocity and water density. Three optional sensors can be added: dissolved oxygen, fluorescence and turbidity.

The CTD-probe, which is battery-driven, is lowered with a wire into the water and was let to take measurements every two seconds. Conductivity, temperature and pressure are used to calculate the salinity and the density. All the data are recorded in physical units and transmitted via a watertight connector. The data are saved on a microchip and can be uploaded in a computer data bank. The benefit of a CTD-sensor is the *in situ* measurement of the parameters. There is no time-lag due to the transporting time to the laboratory, so the sampling with a CTD is very accurate. To be able to compare the dataset from 1916-1993 with the CTD-measured dataset, the depths 0, 5, 10, 20, 30, 40, 50, 60 and 75 meter were analyzed.

Figure 15: CTD/STD - model (SD204 SAIV/ AS, 2014)

3.3 Conversion of oxygen concentration units

Because the oxygen data from 1916-1956 were recorded in different units, a recalculation into SI-units needed to be done. The early oxygen measurements were all measured in [ccm/l], which is equivalent to [ml/l], while the later ones were measured in [mg/l]. For the recalculation of [ml/l] into [mg/l], the molar mass of oxygen (MO_2=31,998 g/mol) and the molar Volume (Vm=22,414 l/mol) are used to create a conversion factor x_{oxygen}.

$$Xoxygen = \frac{31,998\frac{g}{mol}}{22,414\frac{l}{mol}} = 1,428\frac{g}{l} = 1,428\frac{mg}{ml}$$

To be able to get the new value in mg/l it is now required to multiply the available data in ml/l with the conversion factor X_{oxygen}.

$$Ynew\left(\frac{mg}{l}\right) = Yold\left(\frac{ml}{l}\right) * Xoxygen\left(\frac{mg}{ml}\right)$$

4. Results

All hydrographical graphs are modulated using the data attached in Appendix B. All oxygen, water temperature and salinity measurements can be found in Appendix B. The graphs of the Nordic Seas hydrographical measurements are all taken from the "Station Mike" EuroSites homepage (http://www.eurosites.info/stationm.php). The measurements of the NAO winter index are taken from the Climate Data Guide and represent the station based North Atlantic Oscillation Winter Index by Hurrell.

4.1 Hydrographical results of the Barsnesfjord

4.1.1 Salinity
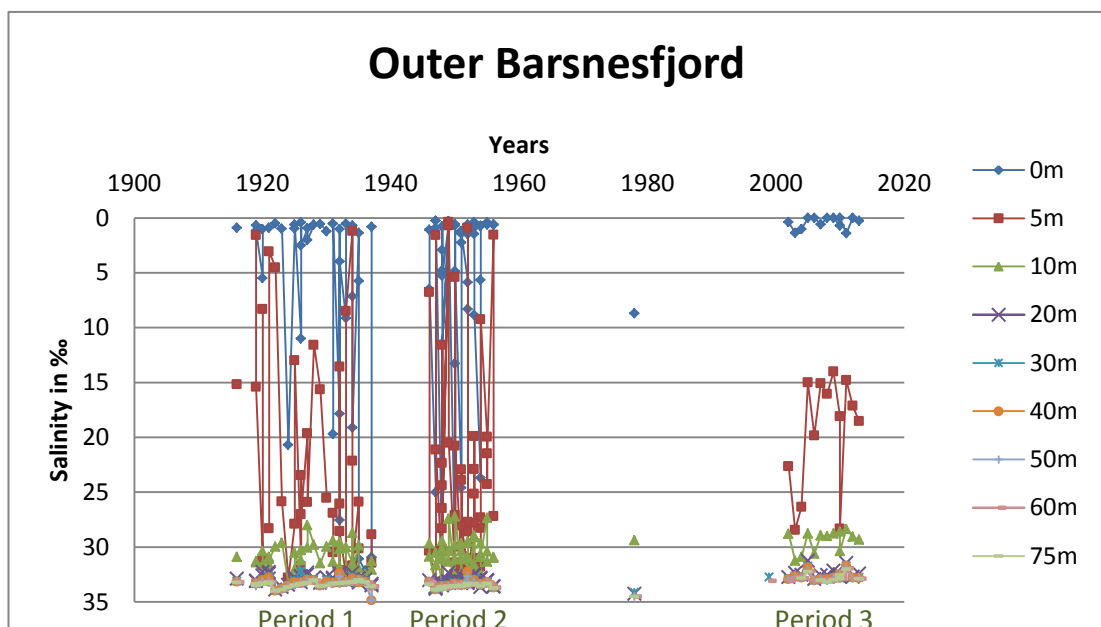
Figure 16: Barsnesfjord, whole dataset for salinity measurements in ‰ from 1916-2013, all depths

Figure 16 shows the whole dataset for the salinity measurements in ‰ over the time period from 1916 till 2013. The fjord sampling can be divided into three time periods. This graph shows the whole dataset with all measured depths to get an overview over the complete set of data of the Outer Barsnesfjord. The x-axis shows the year of sampling, the y-axis illustrates the salinity in ‰ ranging from 0‰ to 35‰. The depths are 0, 5, 10, 20, 30, 40, 50, 60 and 75 meter. It needs to be noted, that the y-axis is reversed, with 0‰ on top and the 35‰ down. It is done this way, to be able to reflect the salinity concentrations in a fjord. Low salinities can be found in the upper layers, the highest salinities in the deepest parts.

The full dataset will be divided and various linked depths will be analyzed individually to get a greater insight in the variability.

Figure 17: Figure 17a shows the whole dataset of the Barsnesfjord for salinity measurements in ‰ from 1916-2013 in the depth of 0 m with measurements throughout the year. Figure 17b depicts the whole dataset of the Barsnesfjord for salinity measurements in ‰ from 1916-2013 in the depth of 0 m with the autumn measurements, namely in August and September.

The 0 meter represents the surface layer (Figure 17a). The wide range of salinity values can be explained with the seasonal variations in precipitation of rain and snow as well as snow melting that lead to great fluctuations in the salt content in the 0 m layer.

The winter values usually hold high salinities, because the freshwater inflow from the river or melt water is extremely low. Figure 17b shows the autumn months of the 0 m, representing the freshwater layer, with values ranging between 0‰ and 10‰. The freshwater input in these months is high, due to snow melt, high precipitation. In the first two periods from 1916-1937 and 1946-1956 great fluctuations in salinity can be seen (Figure 17a). The variations lie between 0‰ and 33‰. These strong fluctuations occur, because the measurements were taken throughout the year. The last period includes only measurements taken every autumn as a part of the "From Mountain To Fjord"-program from 2002-2013. Here the variations are less, since only autumn measurements are available. The range is here from 0‰ to 1.4‰, which are typical salinity values for autumn. Figure 17b shows values only taken in August and September. Here the values range approximately between 0‰ and 3‰, with one spike in 1978, which reaches 8.68‰. Figure 17b shows that the salinity of the 0 m layer in the autumn months has not changed since 1913.
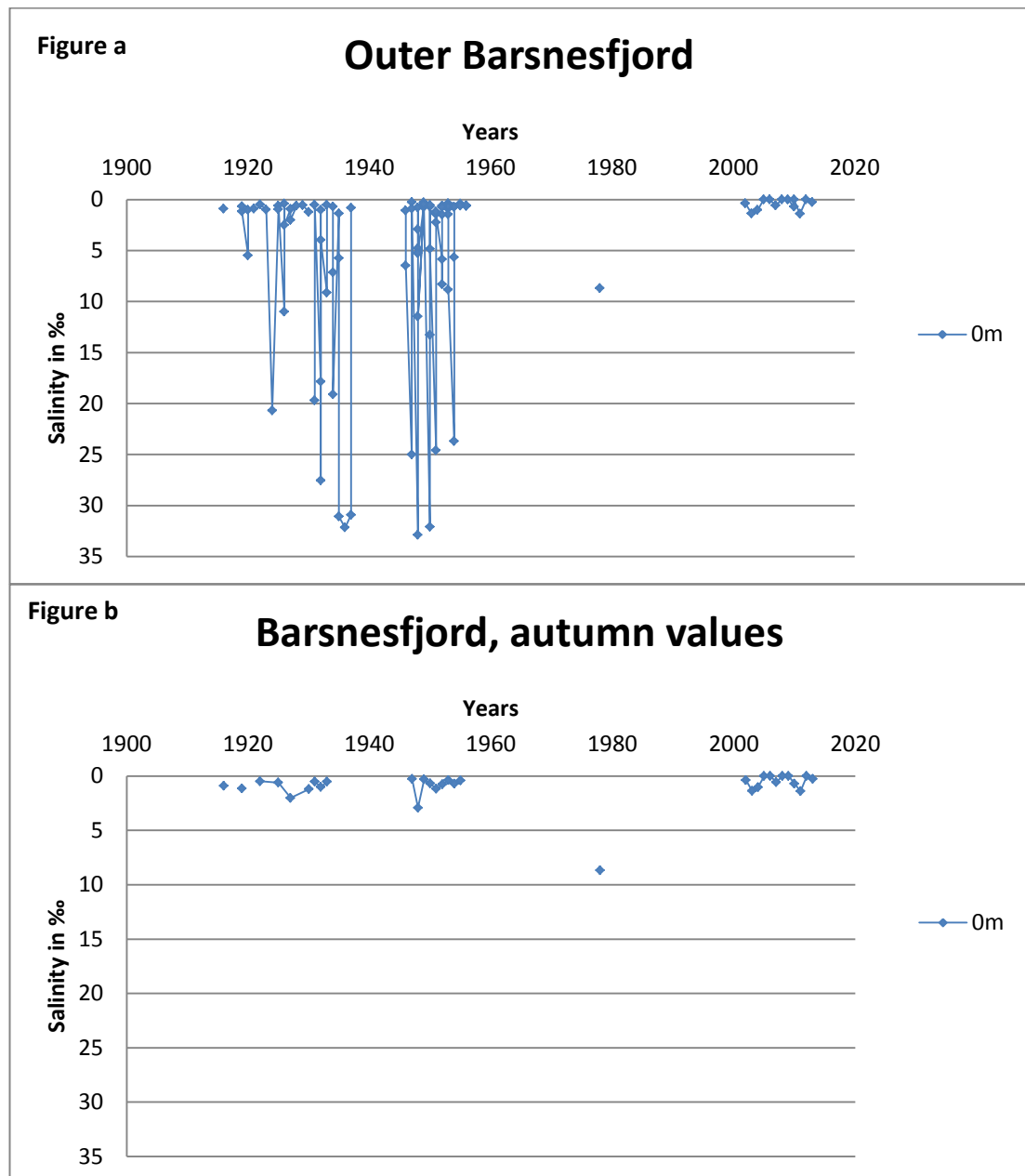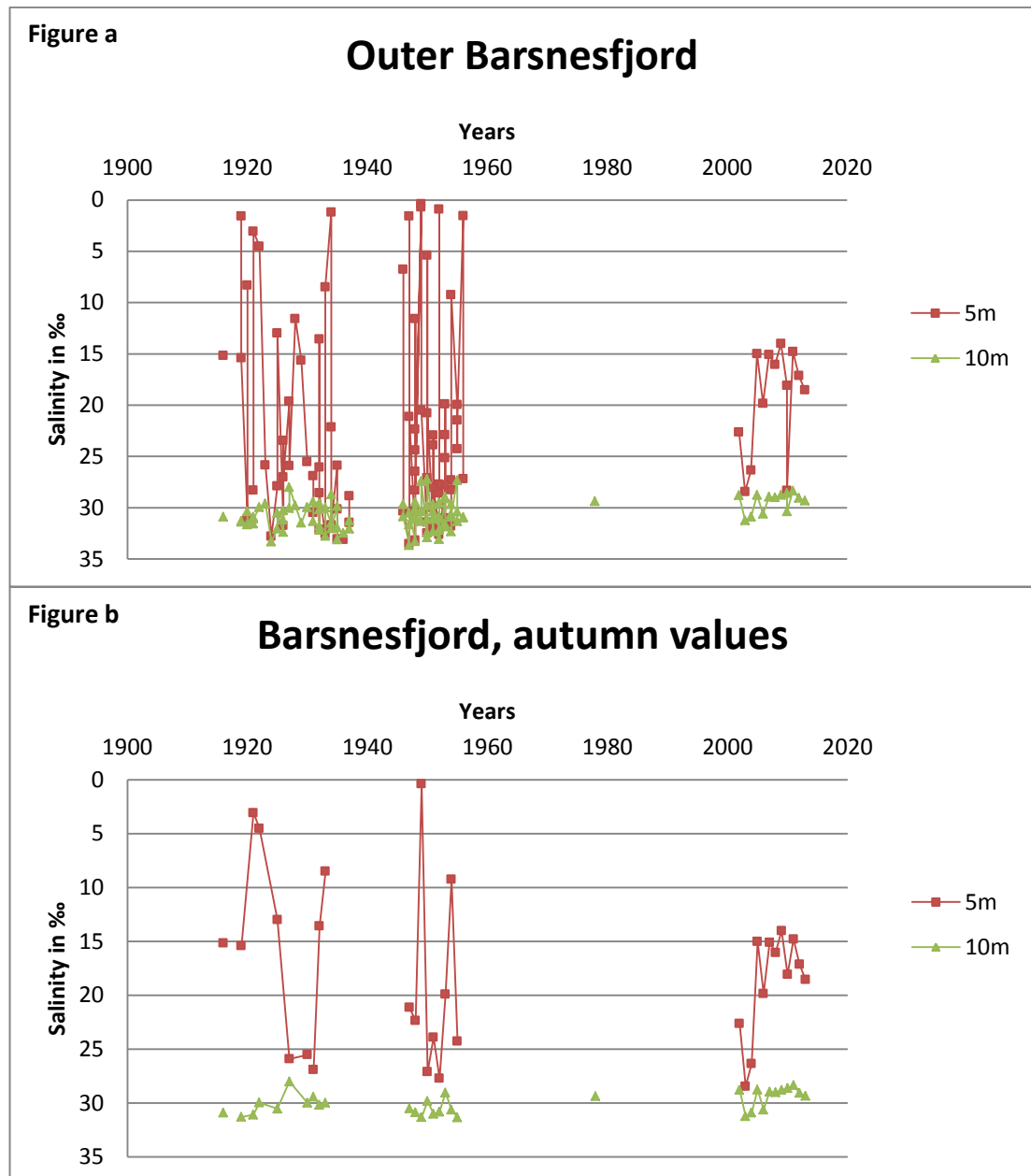
Figure 18: Figure 18a shows the whole dataset of the Barsnesfjord for salinity measurements in ‰ from 1916-2013 in the depth of 5 and 10 m with measurements throughout the year. Figure 18b depicts the whole dataset of the Barsnesfjord for salinity measurements in ‰ from 1916-2013 in the depth of 5 and 10 m with the autumn measurements, namely in August and September.

The 5 and 10 m, being influenced by the surface water, represent the intermediate water layer. In the 10 m layer the differences due to the seasonal variations in salinity cannot be seen as strongly as in the 5 m layer. By comparing Figure 18a and Figure 18b it can be seen that both graphs follow the same pattern of a wide range in the first and second period and a smaller range of salinity variations in the third period for the 5 m layer. At 5 m the values vary between approximately 0.39‰ and 33.19‰ (Figure 18a).

Even in Figure 18b with only autumn values a wide range of salinity values can be seen in the first two periods at 5 m. The 5 m layer is still strongly influenced by the freshwater layer, while the 10 m layer is marked by less influence by the freshwater. The 10 m fluctuate between approximately 27‰ and 33‰ (Figure 18a). The autumn values have a smaller range, with value between 28‰ and 31‰ (Figure 18b).

The last period with measurements that were taken every autumn from 2002-2013 has less variation in the 5 m layer compared to period one and two. These lower fluctuations cannot only be described by the seasonal variations. Figure 18b, showing only autumn values, depicts that in the first two periods the fluctuations were wider than in the third period. There are still periods of high salinity in the third period, but the periods of low salinity have disappeared. A reason for this may be due to the damming in the Sognefjord that was started due to the production of the hydro power plants after the 1960s. Since the dams collect summer water, the fjord received less fresh water in summer time and more freshwater in wintertime. Consequently the 5 m layer is more saline in the autumn month after building of the dams around the Sognefjord and Sogndalsfjord. Since the water of the 5 and 10 m layer is coming from the Sogne- and Sogndalsfjord, all the changes in salinity are also visible in the Barsnesfjord. The range in the 5 m layer in the Barsnesfjord is from approximately 14‰ up to 29‰. The 10 m, ranging between approximately 29‰ and 31‰, are more or less 2‰ less saline than the salinity values from 1916-1956, which fluctuated between 27‰ and 33‰.
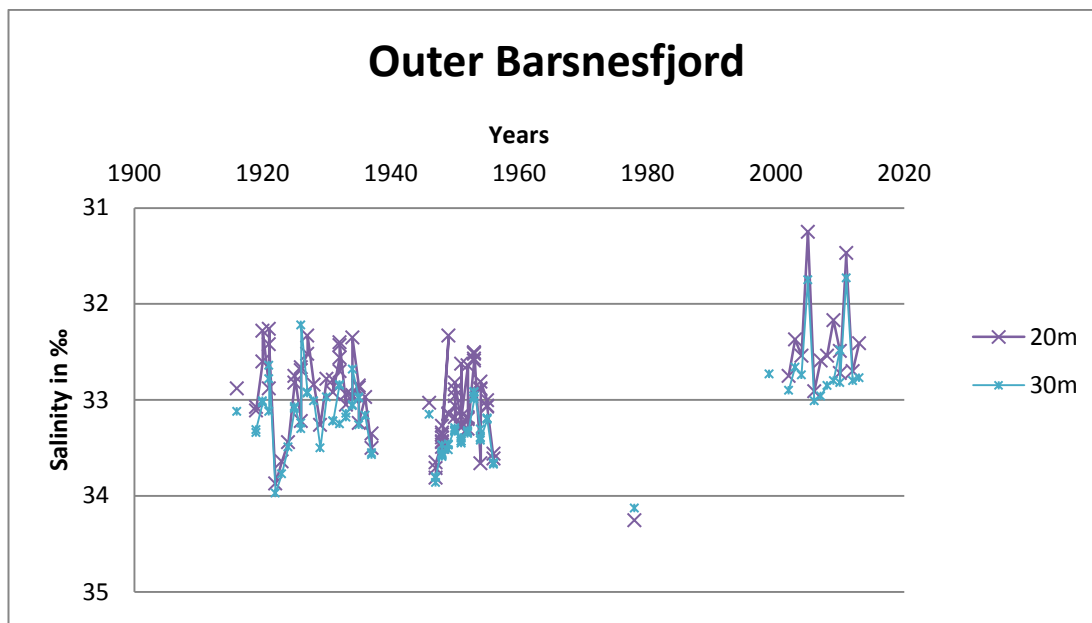
Figure 19: Barsnesfjord, whole dataset for salinity measurements in ‰ from 1916-2013, depths 20m and 30m

In Figure 19 the salinity values of the depths 20 and 30 meter can be seen, representing the upper basin water. These values are less influenced by the surface since they are well below the sill depth of 7.5 m. Changes occurring in these depths could be connected to seasonal variations, inflow events or diffusion and turbulence. The values of the first two periods from 1916-1937 and 1946-1956 mainly range around 32.2‰ and 33.7‰, with the highest salinity values around 34‰ in 1922, 1923 and 1947. The value from 1978 with a measurement of 34.4‰ in the 20 m layer represents the highest salinity value in this record. The measurements from the last period of 2002-2013 show a strong reduction in salinity, with measurements gathering around approximately 32‰ and 33‰. There are two spikes in 2005 and 2011 with extreme low salinities, between 31.25‰ and 31.75‰ in both depths. The basin water of the Barsnesfjord reflects the winter water from the Sogndalsfjord in the depth of 7-20 m. More fresh water is released to the fjords in wintertime due to the dams. It needs to be noted, that the values of 2011 may be not trustworthy, since there might have been a problem with the CTD in this year (Torbjørn Dale, 2014, *personal* communication).
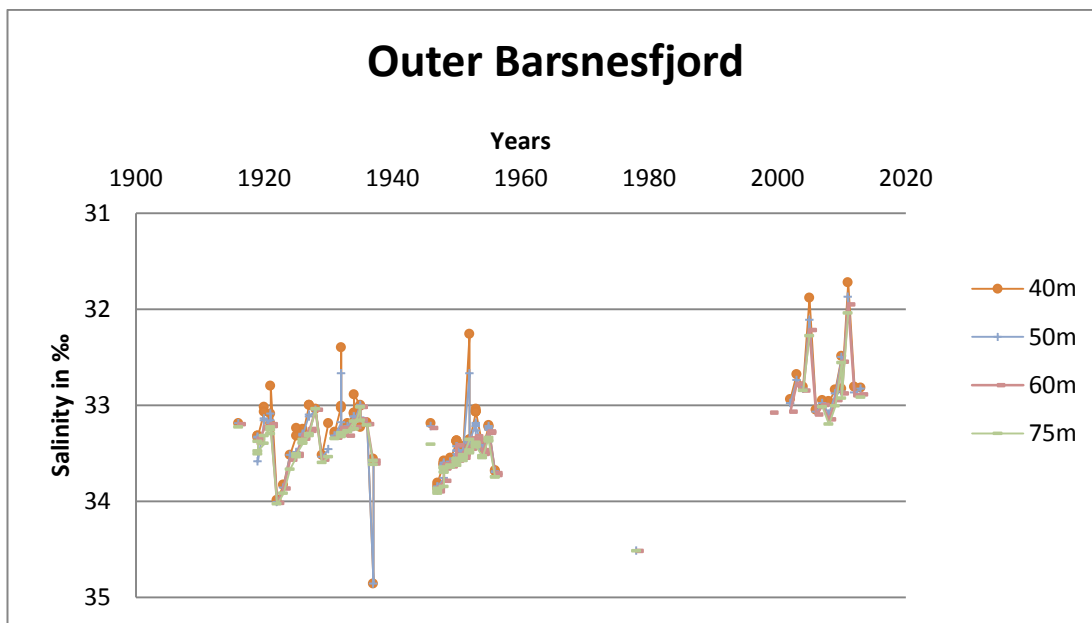
Figure 20: Barsnesfjord, whole dataset for salinity measurements in ‰ from 1916-2013, depths 40, 50, 60 and 75m

Figure 20 shows the salinity values of the depths 40, 50, 60 and 75 meter. These depths are the deep basin water and are little influenced by the intermediate water due to diffusion and turbulence. The values from the two first periods from 1916-1937 and 1946-1956 mainly range between 33‰ and 34‰, although there three spikes with lower salinities at 40 m, namely 32.8‰ in 1921, 32.4‰ in 1932 and 32.26‰ in 1952. There is one spike with the highest salinity values represented in this record in 1937 with values of 34.86‰ in both 40 and 50 m. The values from 1978 are all in the range of 34.5‰ and are, aside from the spike in 1937 with values of 34.86‰, the highest values of the record. The measurements from 2002-2013 show a strong fall in salinity. Those measurements gather around approximately 32‰ and 33‰, with two spikes in 2005 and 2011 with lower salinities in all four depths. The basin water of the Barsnesfjord reflects the winter water from the Sogndalsfjord in the depth of 7-20 m. More fresh water is released to the fjords in wintertime due to the dams. Comparing the first two periods of 1916-1956 with values between 33‰ and 34‰ with the last period with values ranging between 32‰ and 33‰, an overall drop in salinity of approximately 1‰ can be established.

4.1.2 Temperature
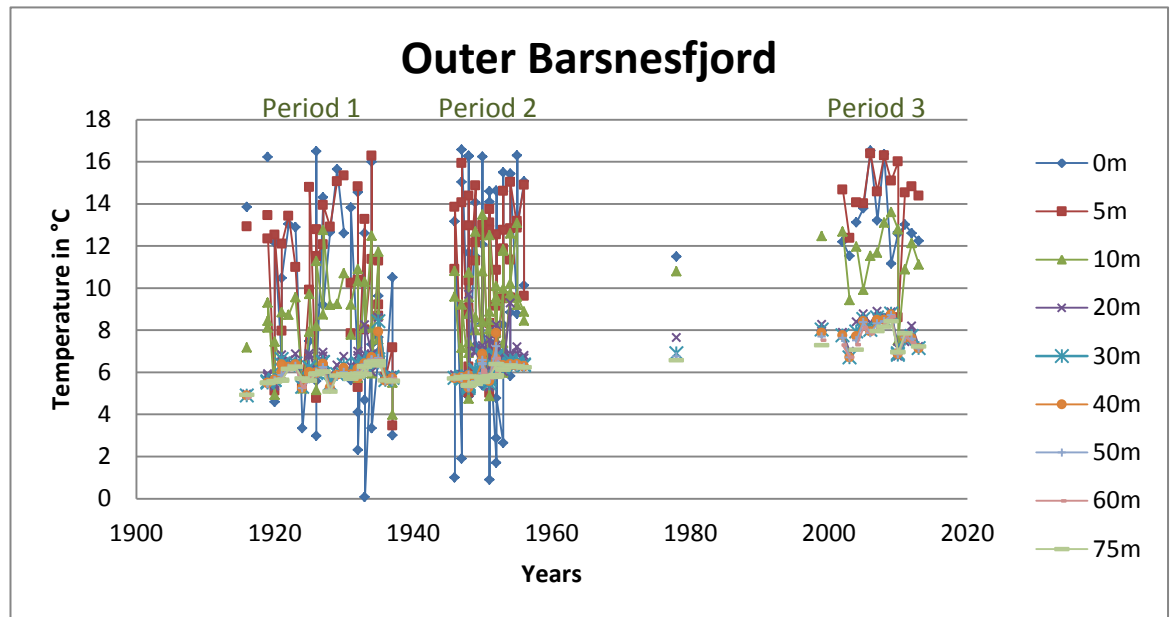
Figure 21: Barsnesfjord, whole dataset for temperature measurements in °C from 1916-2013, all depths

Figure 21 shows the whole dataset for the temperature measurements in °C over the time span from 1916 till 2013. As in the salinity values, the fjord sampling can be divided into three time periods. This graph shows the whole dataset with all measured depths to again get an overview over the complete set of data of the Outer Barsnesfjord. The x-axis shows the year of sampling, the y-axis illustrates the temperature in °C ranging from 0°C to 18°C. The depths are 0, 5, 10, 20, 30, 40, 50, 60 and 75 meter. Even in this first graph with too much information to be analyzed properly, a general rise in temperature can be easily seen. As done before with the salinity data, the full dataset will be divided and various linked depths will be analyzed separately to get a greater insight into the variability.

Figure 22: Figure 22a shows the whole dataset of the Barsnesfjord for temperature measurements in °C from 1916-2013 in the depth of 0m with measurements throughout the year. Figure 22b depicts the whole dataset of the Barsnesfjord for temperature measurements in °C from 1916-2013 in the depth of 0m with the autumn measurements, namely in August and September.

The 0 meter represents the surface layer, which contains melt water from the glacier, snowmelt, the river water from the Årøyelv and precipitation. The upper layer holds a wide range of temperature, due to seasonal variations in insolation and the surrounding air temperature, which directly influences the 0 m layer. In the two first periods from 1916-1937 and 1946-1956 the widest fluctuations can be seen (Figure 22a). The values lie between 0.08°C and 16.57°C. These measurements were taken throughout the year and thus reflect spring, summer, autumn and

winter air temperatures. The last period includes only measurements taken every autumn from 2002-2013. Here the variations are less, since they include only one season. The range is here from 11.16°C to 16.54°C. Figure 22b, which depicts the autumn values, namely from August and September, shows a smaller range of temperatures in the 0 m layer, mainly ranging between 12°C and 16°C, with two lower values in 1921 with 10.48 °C and in 1927 with 9.2°C. From the first to the second period an increase in temperature can be depicted. From the second to the third period the temperature values decrease again, which may be due to glacial melting. Also the inlet water to the hydroelectric power plant in Årøy, which is coming from Lake Hafslo through a tunnel, might be connected to the cooling. Usually the water would be heated up by the atmosphere on its way in the river to the fjord. This is now not possible, since it is kept cold in the tunnel. It cannot easily be said, which of these possible explanations are responsible for the cooling.
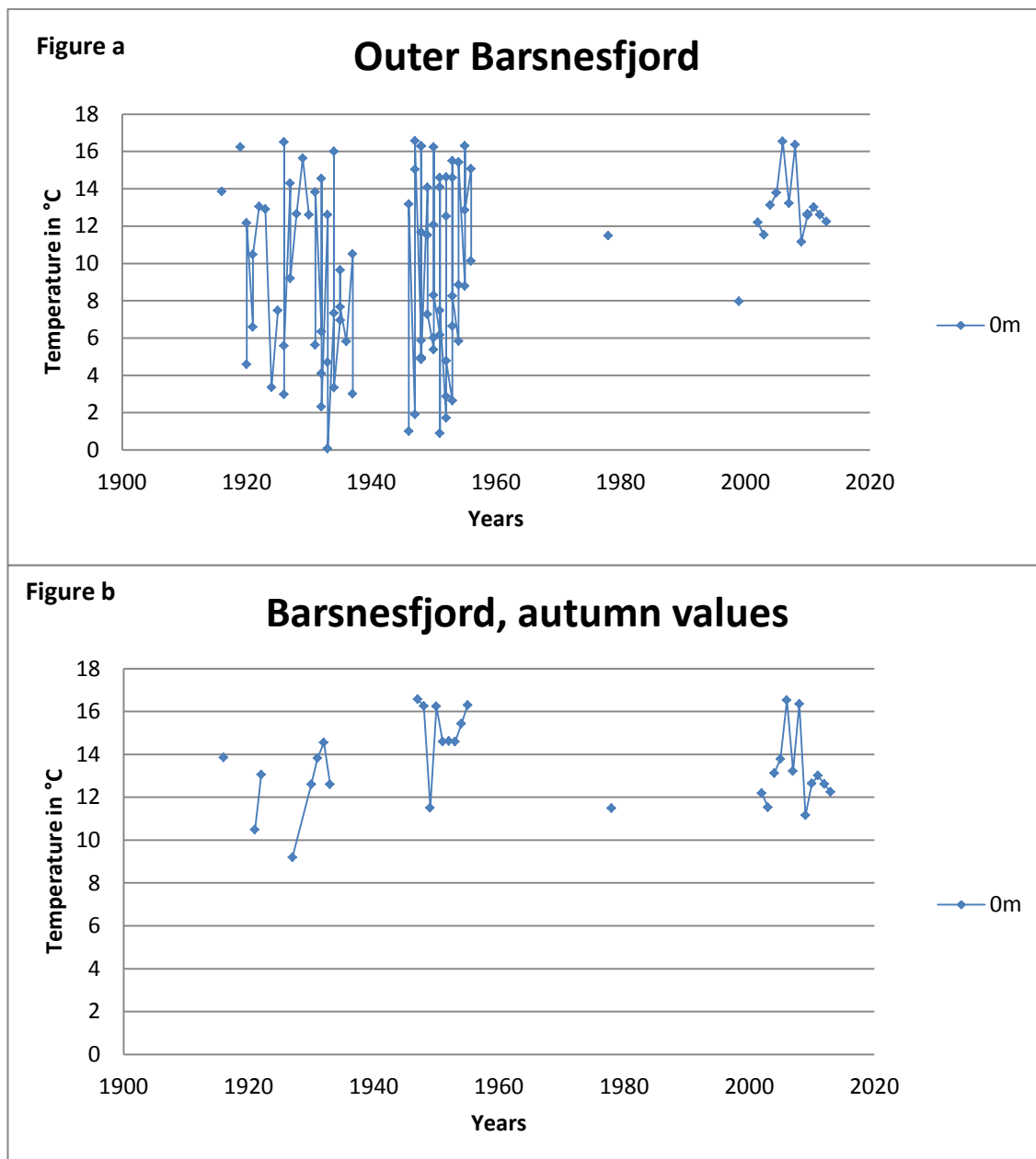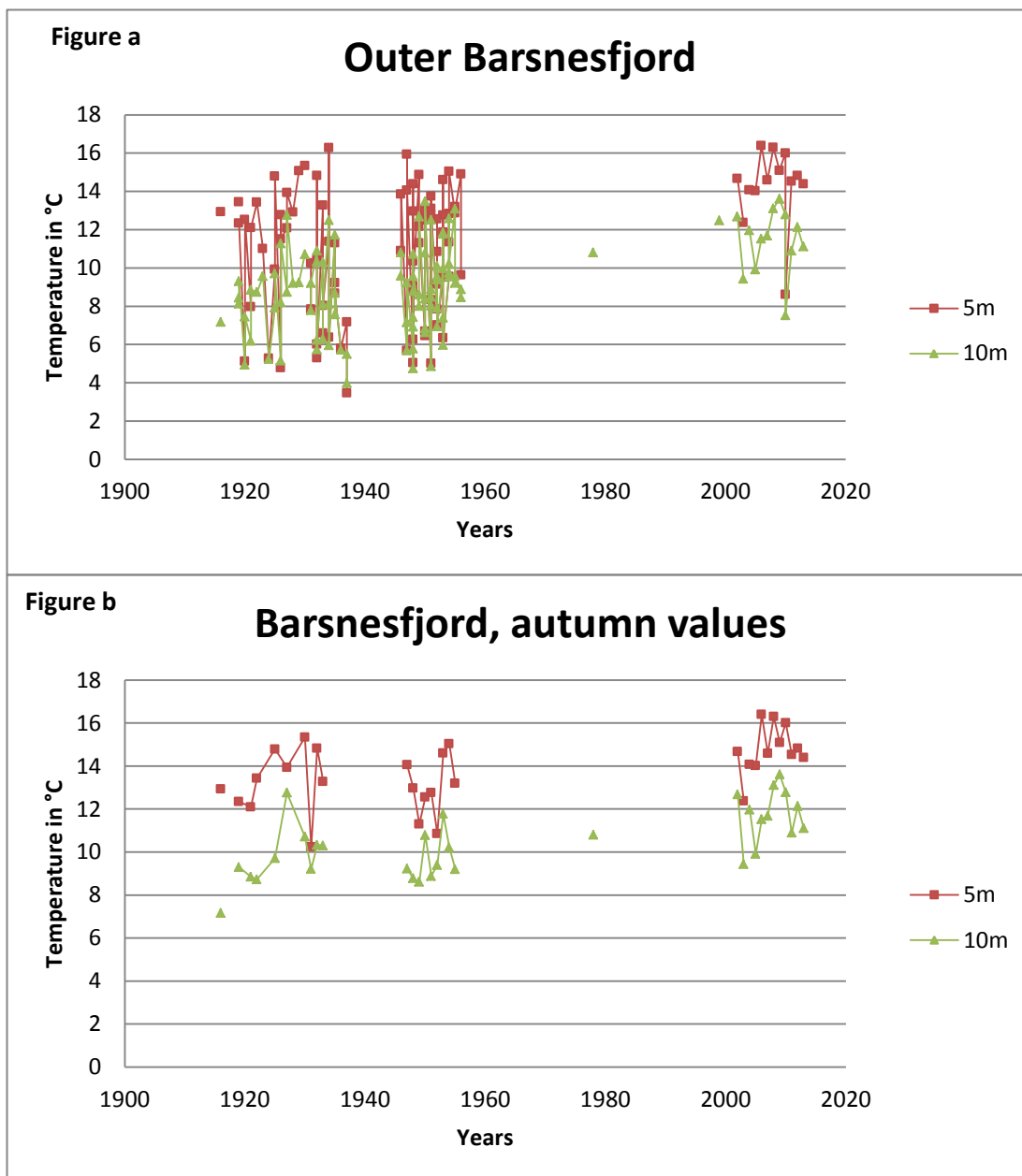
Figure 23: Figure 23a shows the whole dataset of the Barsnesfjord for temperature measurements in °C from 1916-2013 in the depth of 5 and 10 m with measurements throughout the year. Figure 23b depicts the whole dataset of the Barsnesfjord for temperature measurements in °C from 1916-2013 in the depth of 5 and 10 m with the autumn measurements, namely in August and September.

The 5 and 10 m represent the intermediate water layer and are influenced by the surface water and thus the seasonal variations in air temperature. In the two first periods from 1916-1937 and 1946-1956 there are again the widest fluctuations (Figure 23a).

These strong fluctuations can be explained by the seasonal differences in insolation and the surrounding air temperature which directly influence the 5 m and 10 m via surface currents and diffusion. The values vary between approximately 5°C and 15°C. These measurements were taken throughout the year and thus reflect all seasons air temperatures and insolation rates, which influence the upper layers. The temperatures do not reach the 0°C as in the 0 m. The lowest temperature measured at 5 m was 3.47°C in 1937. The last period from 2002- 2013, has fewer variations, since only one season was looked at. The range is here from approximately 9°C up to 16°C.

To be able to identify a "warming trend" in the depths of 5 and 10 m, it is necessary to look at Figure 23b, which shows only the autumn values from August and September, when the water temperatures have reached their highest value due to solar irradiation. In Figure 23b a warming trend can be determined, which cannot only be explained by seasonal changes. This warming trend could be caused by the dams that store the cold summer river water. The great amount of cold river water that is normally added to the fjord in summertime in a now regulated river is minimized due to the saving of the water in dams for the production of hydroelectric power. This reduction in cold water inflow from the river could explain the increase in the temperature in the 5 and 10 m layer of the Barsnesfjord. Also the general warming trend, which can be seen in the basin water, could be connected to this temperature increase.
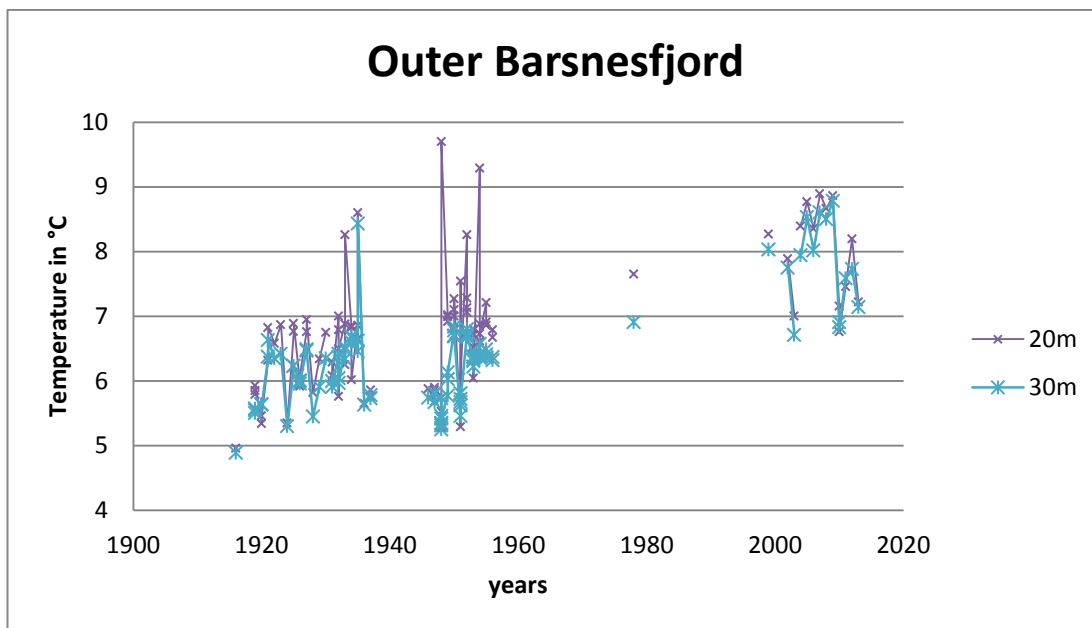
Figure 24: Barsnesfjord, whole dataset for temperature measurements in °C from 1916-2013, depths 20 m and 30 m

Figure 24 shows the temperature values from the depths 20 and 30 meter, representing the upper basin water. The temperature values of these depths are less influenced by the surface since they are well below the sill depth of 7.5 m. Changes occurring in these depths could be connected to seasonal variations, inflow events or diffusion and turbulence. The values from the first two periods from 1916-1937 and 1946-1956 mainly range around 5°C and 7°C, although there are some spikes in the 20 m layer, that are out of line and do not fit the pattern of the temperature values of the 30 m layer. There are values that even almost reach the 10°C at a 20 m depth. The highest value of 9.7°C was taken in December and represents the summer heat pulse of the warm surface waters, which reach the deeper parts later in the year, namely in December. Other values with similar high temperatures at 20m were also from December or October. Comparing the two first periods with the third period from 2002-2013 a rise in the temperature can clearly be seen. The lowest value reached is 6.71°C in 2003 at 30m depth. The basin water of the Barsnesfjord reflect the winter temperatures from the Sogndalsfjord in the depth of 7-20 m. The measurements from the last period from 2002-2013 vary between 7°C and 9°C. Comparing these values with the values from the first period of 1916-1956, mainly ranging around 5°C and 7°C, a rise of approximately 2°C can be determined.
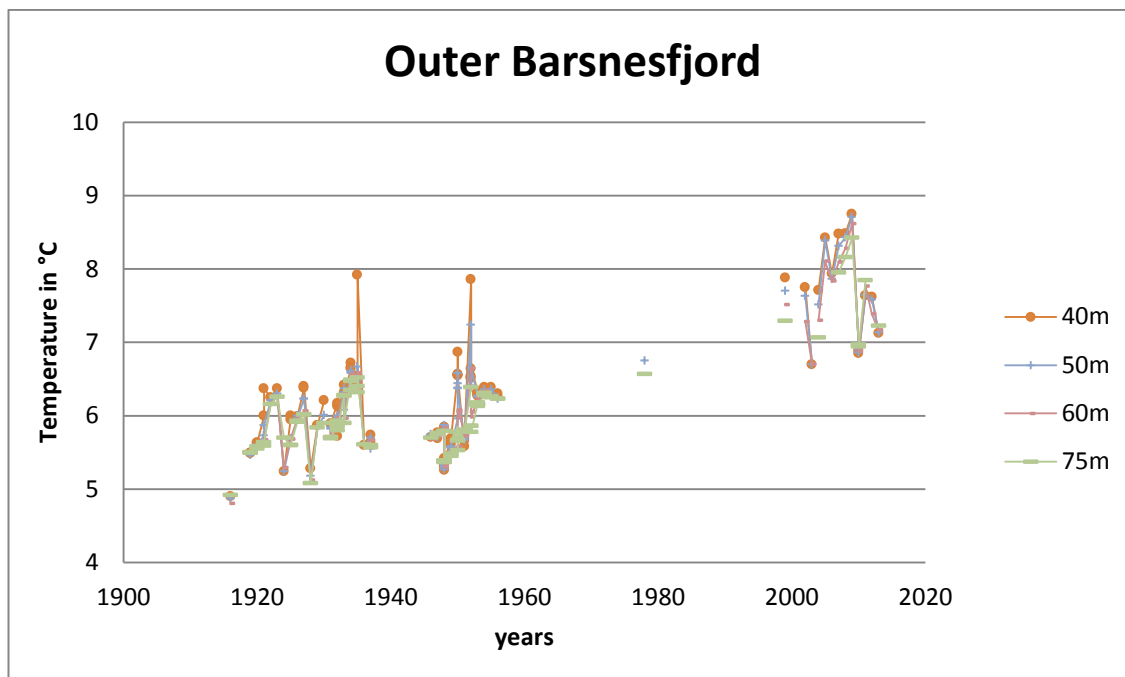
Figure 25: Barsnesfjord, whole dataset for temperature measurements in °C from 1916-2013, depths 40, 50, 60 and 75m

Figure 25 shows the temperature values of the depths 40, 50 60 and 75 meter depths. These depths are the deep basin water and are little influenced by the intermediate water due to diffusion and turbulence. They are also below the 29 m sill between Inner and Outer Barsnesfjord. The values from the first two periods from 1916-1937 and 1946-1956 mainly range around 5°C and 6.5°C, although there are some spikes that are higher than the other values. The two highest values are 7.92°C in January 1935 and 7.86°C in December 1952, which may represent the summer heat pulse of the warm surface waters, which reach the deeper parts later in the year, namely in January and December. From 1978 till 2013 a rise in temperature can be observed. The lowest temperature in this deep basin water was found in 1916 with 4.8°C at 60m. Comparing it now to the last period from 2002-2013, the lowest measured values is also at 60 m, but it lies at 6.7°C and was taken in 2003. This is a difference of 1.9°C. The measurements from 2002 to 2013 lay between approximately 7°C and 9°C. When we again compare these values with the values from the first period of 1916-1956, which were mainly concentrating between 5°C and 7°C, a rise of around 2°C can be established.

4.1.3 Oxygen
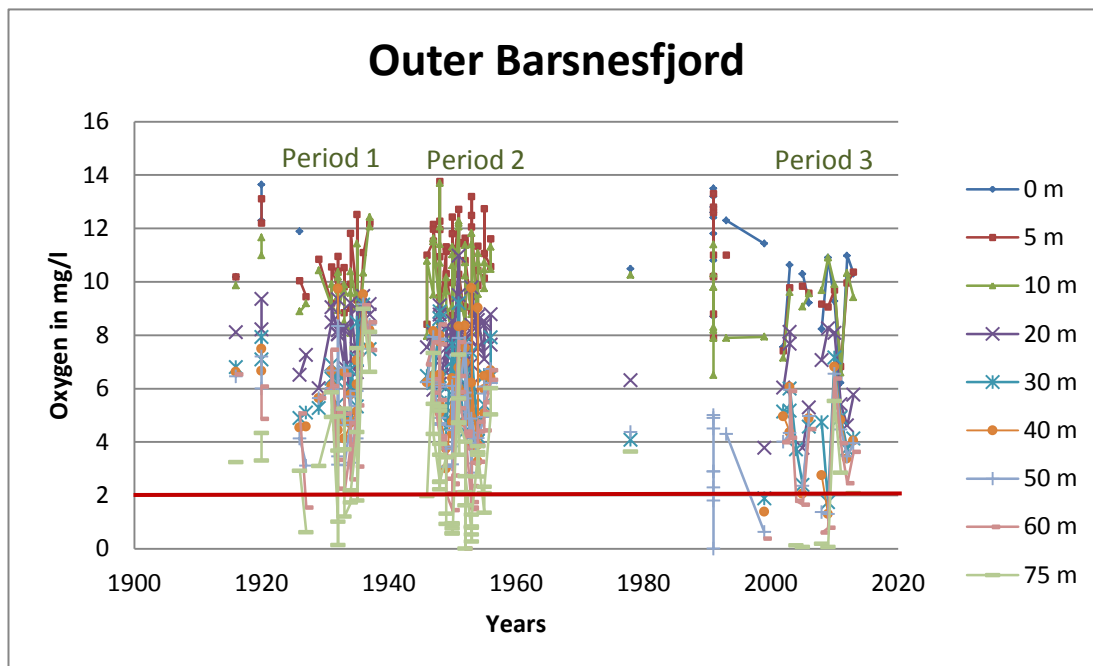
Figure 26: Barsnesfjord, whole dataset for oxygen measurements in mg/l from 1916-2013, all depths. The red line at 2 mg/l illustrates the critical oxygen level.

Figure 26 shows the whole dataset for the oxygen measurements in mg/l of the time period from 1916 till 2013. The fjord sampling can be divided into three time periods. This first oxygen graph shows the whole dataset with all measured depths to get an overview over the complete set of data of the Outer Barsnesfjord. Subsequently the full dataset will be divided and various linked depths will be analyzed individually to get a greater insight into the variations. The x-axis shows the year of sampling, the y-axis illustrates the oxygen in mg/l ranging from 0 mg/l to 16 mg/l. The depths are 0, 5, 10, 20, 30, 40, 50, 60 and 75 meter.
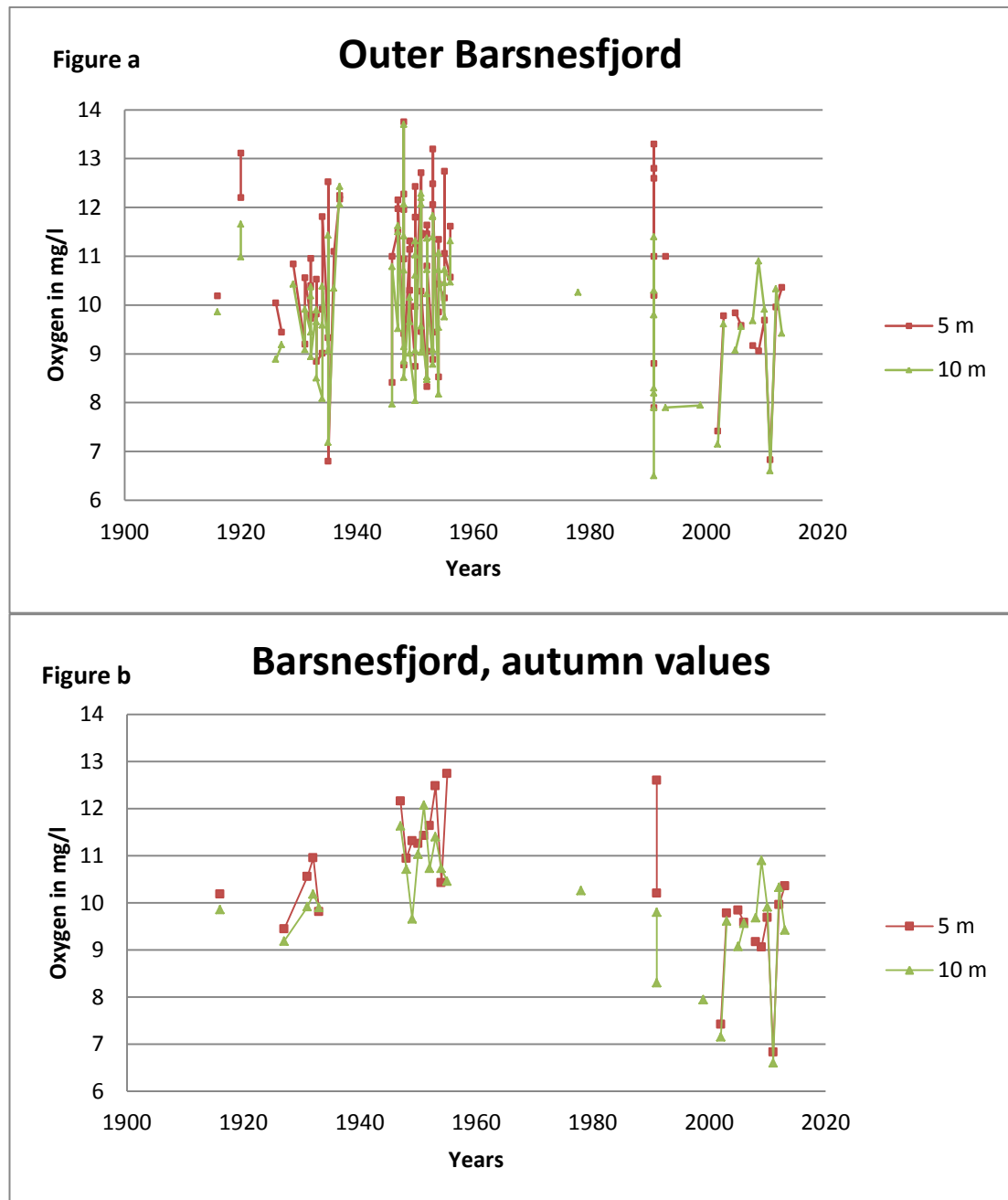
Figure 27: Figure 27a shows the whole dataset of the Barsnesfjord for oxygen measurements in mg/l from 1916-2013 in the depth of 5 and 10 m with measurements throughout the year. Figure 27b depicts the whole dataset of the Barsnesfjord for oxygen measurements in mg/l from 1916-2013 in the depth of 5 and 10 m with the autumn measurements, namely in August and September.

Since the oxygen data in the Outer Barsnesfjord from 1916-2013 in the 0 meter depth is incomplete and includes only few measurements, it will be left out and won´t be described closer. The data for the 5 and 10 meter on the other hand are more complete and thus will be described. The 5 and 10 meter can be counted to the intermediate water layer. It is also in the euphotic zone in which oxygen is produced from photosynthesis.

In the first two periods from 1916-1937 and 1946-1956 the oxygen concentrations vary mainly between 8 mg/l and 13 mg/l with one spike in 1935 with less than 7 mg/l (Figure 27a). In the last period from 2002-2013, with only autumn measurements, it can be seen, that the oxygen values have dropped. The maximum oxygen value does not even reach 11 mg/l. The lowest value is 6.6 mg/l, which could be an underestimation.

When only analyzing the autumn values in Figure 27b, an overall reduction in oxygen values can be seen, especially when comparing the third period with values between 6.6 mg/l and 10.9 mg/l with the second period with values between 9.66 mg/l and 12.74 mg/l. This drop at 5 and 10 m could be related to the temperature increase that can be seen in the same depths of 5 and 10 m (Figure 23). With a temperature increase, which could partly be caused by the decreased adding of cold river water to the fjord due to dams and the general temperature increase, the oxygen concentrations are reduced. This happens because the water cannot hold as much oxygen at high temperatures and because the biological respiration increases, which leads to a higher oxygen consumption. Another possible factor for the oxygen decrease in the 5 and 10 m layer might be the eutrophication of the fjords, as well as of the Nordic Seas. Eutrophication might cause increased oxygen consumption from increased food supply.
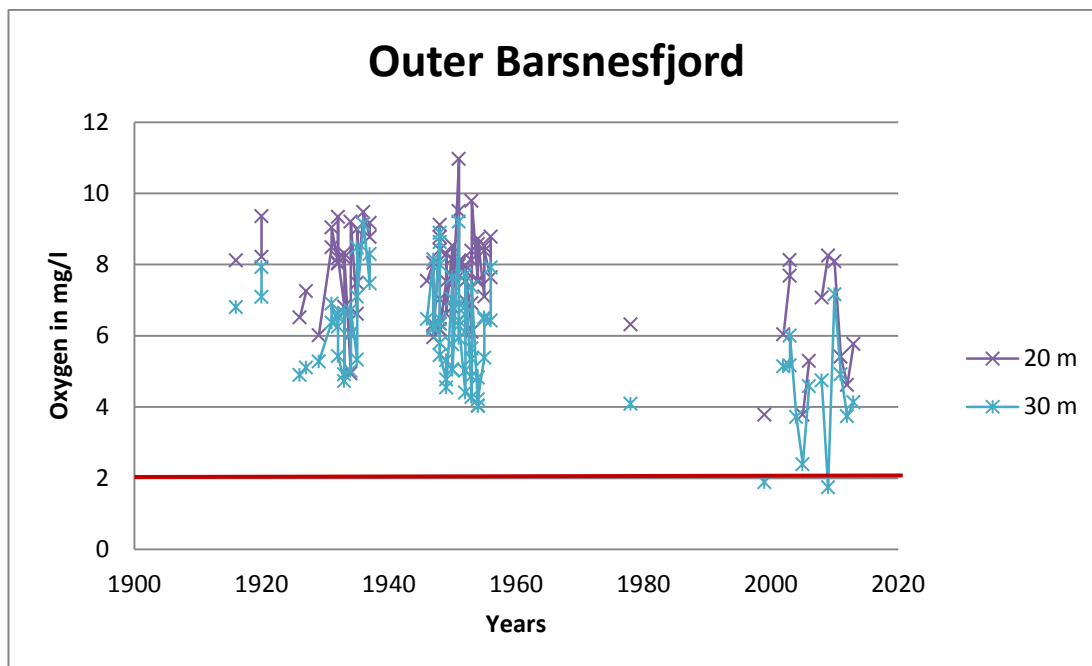
Figure 28: Barsnesfjord, dataset for oxygen measurements in mg/l from 1916-2013, depths 20 and 30 meter. The red line at 2 mg/l illustrates the critical oxygen level.

Figure 28 shows the oxygen values of the depths 20 and 30 meter. The temperature values of these depths are less influenced by the surface since they are well below the sill depth of 7.5 m. Changes occurring in these depths could be connected to seasonal variations, inflow events or diffusion and turbulence. Theses depths can be described as the upper basin water. In these depths the drop in oxygen can be seen even clearer than at 5 and 10 m. In the two first periods from 1916-1937 and 1946-1956 the oxygen concentration varies mainly between 4 mg/l and 10 mg/l with one spike in 1951 with approximately 11 mg/l. In 1999 the first killing event happened with oxygen concentrations of 1.89 mg/l in the 30 m water layer. In the last period from 2002-2013 the critical oxygen concentration of 1.74 mg/l was reached in 2009 at 30 m. The highest values were only around 8 mg/l which is markedly lower than the highest values in the period from 1916-1956 of around 10 mg/l. Minimum and maximum values were both lower in the third period compared to the two first periods.
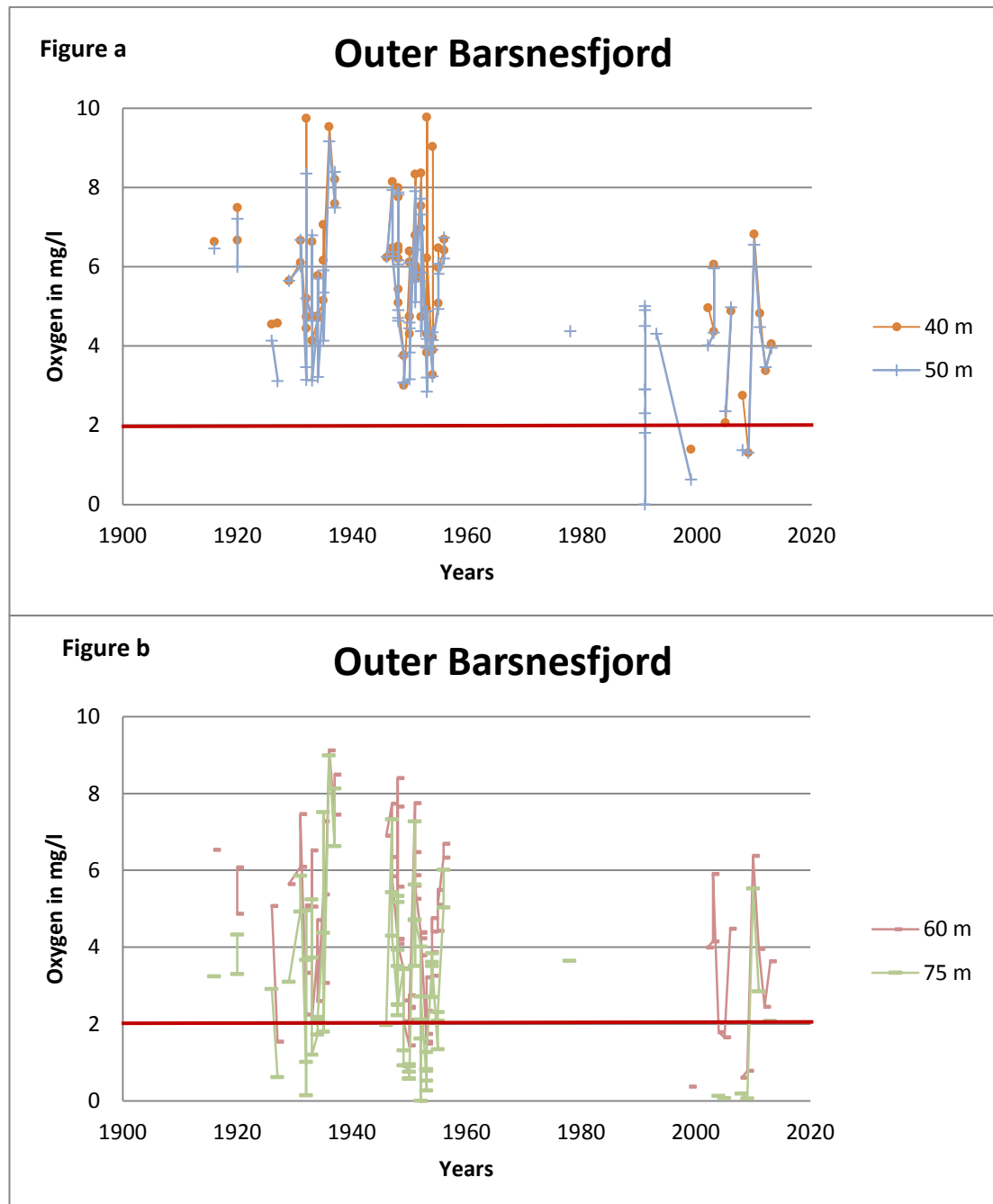
Figure 29: Figure 29a shows the whole dataset for oxygen measurements in mg/l from 1916-2013 of the Barsnesfjord in the depths 40 and 50 m. Figure 29b shows the whole dataset for oxygen measurements in mg/l from 1916-2013 of the Barsnesfjord in the depths 60 and 75 m. The red line at 2 mg/l illustrates the critical oxygen level.

Figure 29 shows the depths of the basin water, namely 40 and 50 m in Figure 29a and 60 and 75 m in Figure 29b. For the depths 60 and 75 m values between 0 mg/l and 2 mg/l are frequently reached in all periods (Figure 29b). The highest concentrations are reached in the first periods, reaching up to 9 mg/l. The third period values do not reach these high values. The highest oxygen concentration in the third period can be found in 2010 with only 6.37 mg/l.

At the depths of 40 and 50 m (Figure 29a) the two first periods hold oxygen concentrations between 3 mg/l and 10 mg/l and concentrations below the critical oxygen level of 2 mg/l are never reached in period one and two. Only in the third period the suboxic conditions, that can be seen in all three periods for the 60 and 75 m layer. These suboxic conditions reach the depths of 40 and 50 m frequently, namely in 1991, 1999 and 2009 and almost in 2005. Even the depth of 30 m reached critical oxygen concentrations of 1.89 mg/l in 1999 and 1.74 mg/l in 2009 (Figure 28).

These episodic bad conditions in the third period at 30, 40 and 50 m may be caused by temperature increase and therefore an increased respiration leading to a decrease in oxygen concentration in the water. Another possibilities may be a decrease in the inflow frequency, the infilling of the Loftesnes bridge, as well as a possible increased supply of sewage to the Sogndalsfjord brought into the Barsnesfjord by the intermediate water exchange.

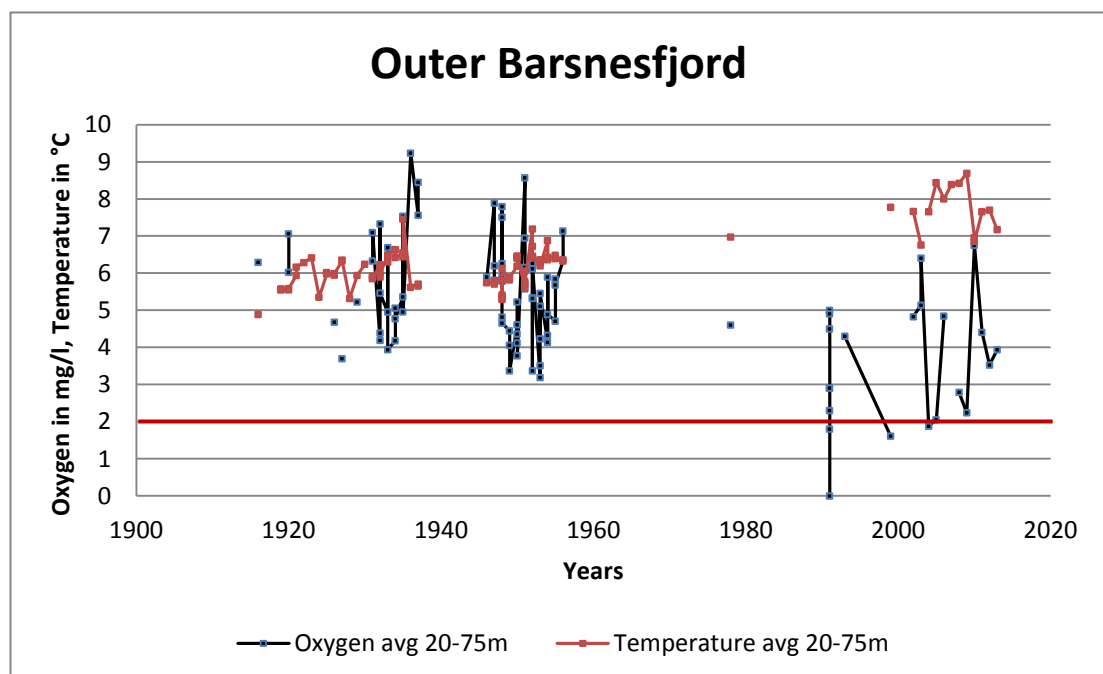### 4.1.4 Comparison of Oxygen and Temperature values in the Barsnesfjord

Figure 30: Barsnesfjord, whole dataset for Oxygen measurements in mg/l in black and temperature measurements in ° C in red from 1916-2013, average for the deeper depths 20, 30, 40, 50, 60 and 75 m. An overall increase in temperature and an overall decrease in oxygen can be seen. The red line at 2 mg/l illustrates the critical oxygen level.

Figure 30 shows oxygen and temperature values of the Barsnesfjord from 1916-2013 running against each other. To compare it better, the surface influenced depths of 0, 5 and 10 m were left out and the averages of 20, 30, 40, 50, 60 and 75 m were calculated. Colder water can hold more oxygen than warm water, which makes temperature and oxygen to inversely correlating parameter. With increasing water temperatures also the oxygen consumption increases, which also strengthens the inverse correlation between temperature and oxygen content. In the first two periods from 1916-1937 and 1946-1956 the oxygen and temperature values fluctuate in a similar range. Oxygen values lie between 3 mg/l and 9 mg/l, temperature values between 5°C and 7°C. After 1956 both parameters oxygen and temperature run away from each other. While temperature increases up to a range between 7°C to 9°C, the oxygen values decrease to values ranging between 0 mg/l and 7 mg/l, reaching the critical oxygen level of 2 mg/l three times in 1991, 1993 and 2004.

4.1.5 Inflow Years Barsnesfjord

To point out the inflow years in the Barsnesfjord, it is reasonable to take a closer look at the oxygen values of the three main periods of measurements. The first period is from 1916-1937, the second from 1946-1956 and the third from 2002-2013. To get a better insight into the oxygen variations the same pattern of dividing the full data set into different depths will be continued. The depths are 20 and 30 m, representing the upper basin water and 40, 50, 60 and 75 m, representing the deeper basin water. Especially for the deep basin water, the inflow years can be easily identified. When there is a rise in oxygen, an inflow of new water into the basin is occurring. For the intermediate layer, namely the 5 and 10 m, other factors are relevant for the increase in oxygen, namely photosynthesis, thermohaline circulation, salinity, insolation and as a result the water temperature as well as disposal of waste water.

Figure 31: Oxygen values of the Barsnesfjord from 1916-1937, 1946-1956 and 2002-2013 in the depths of 20 and 30m showing the inflow years. First period has inflows every year, second period has inflows every year and third period has inflows every 3-4 years, namely in 2006, 2010 and 2013. There might have been more inflows between 2006 and 2008, which cannot be located since there is one year of measurements missing.

Figure 32: Oxygen values of the Barsnesfjord from 1916-1937, 1946-1956 and 2002-2013 in the depths of 40 and 50m showing the inflow years. First period has inflows every year, second period has inflows every year and the third period has inflows every 3-4 years, namely in 2006, 2010 and 2013. There might have been more inflows between 2006 and 2008, which cannot be located since there is one year of measurements missing.

Figure 33: Oxygen values of the Barsnesfjord from 1916-1937, 1946-1956 and 2002-2013 in the depths of 60 and 75m showing the inflow years. First period has inflows every year; the second period has inflows every 1-3 years, namely in 1947, 1948, 1951, 1954, 1955 and 1956. The third period has inflows every 3-4 years, namely in 2006, 2010 and 2013. There might have been more inflows between 2006 and 2008, which cannot be located since there is one year of measurements missing.
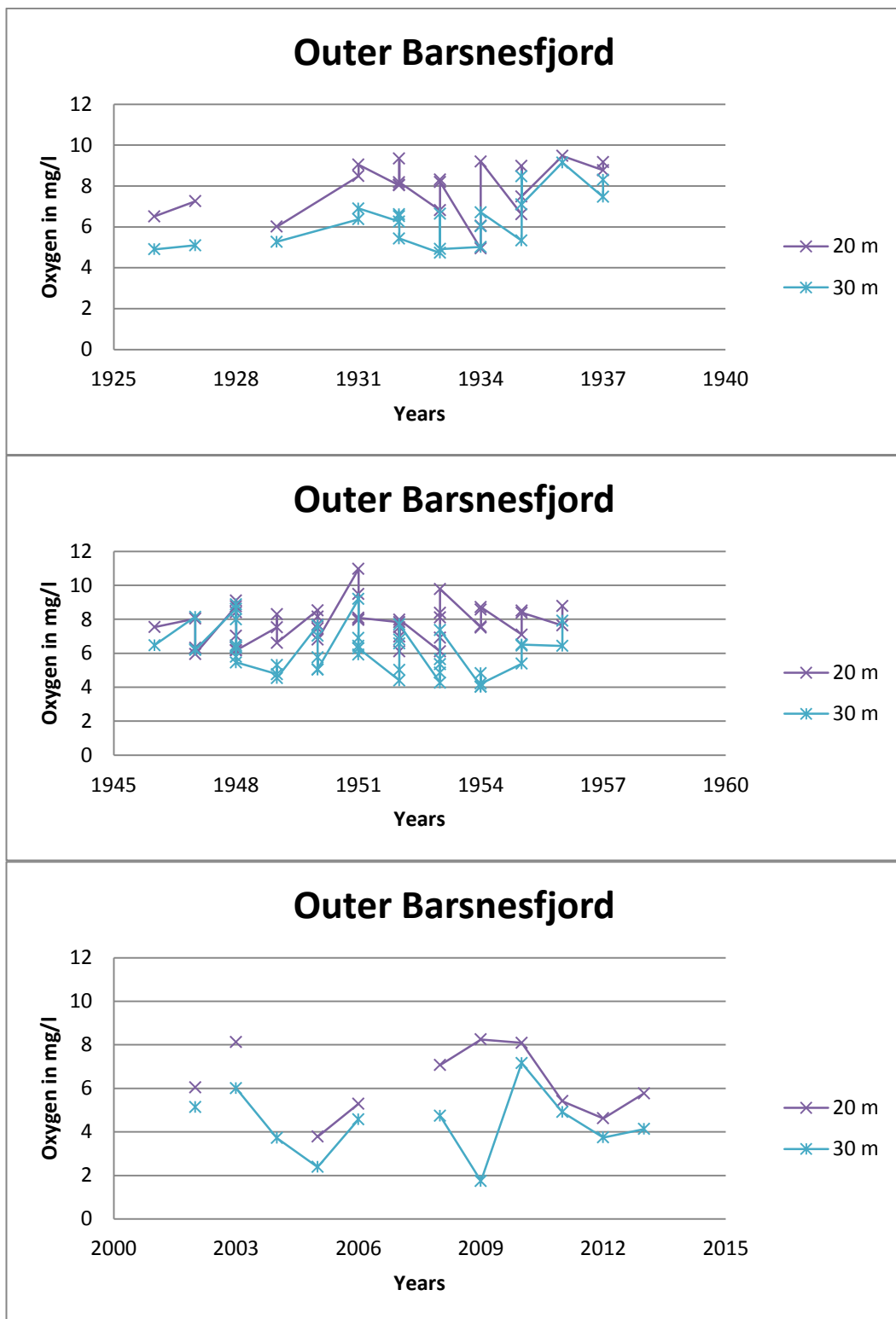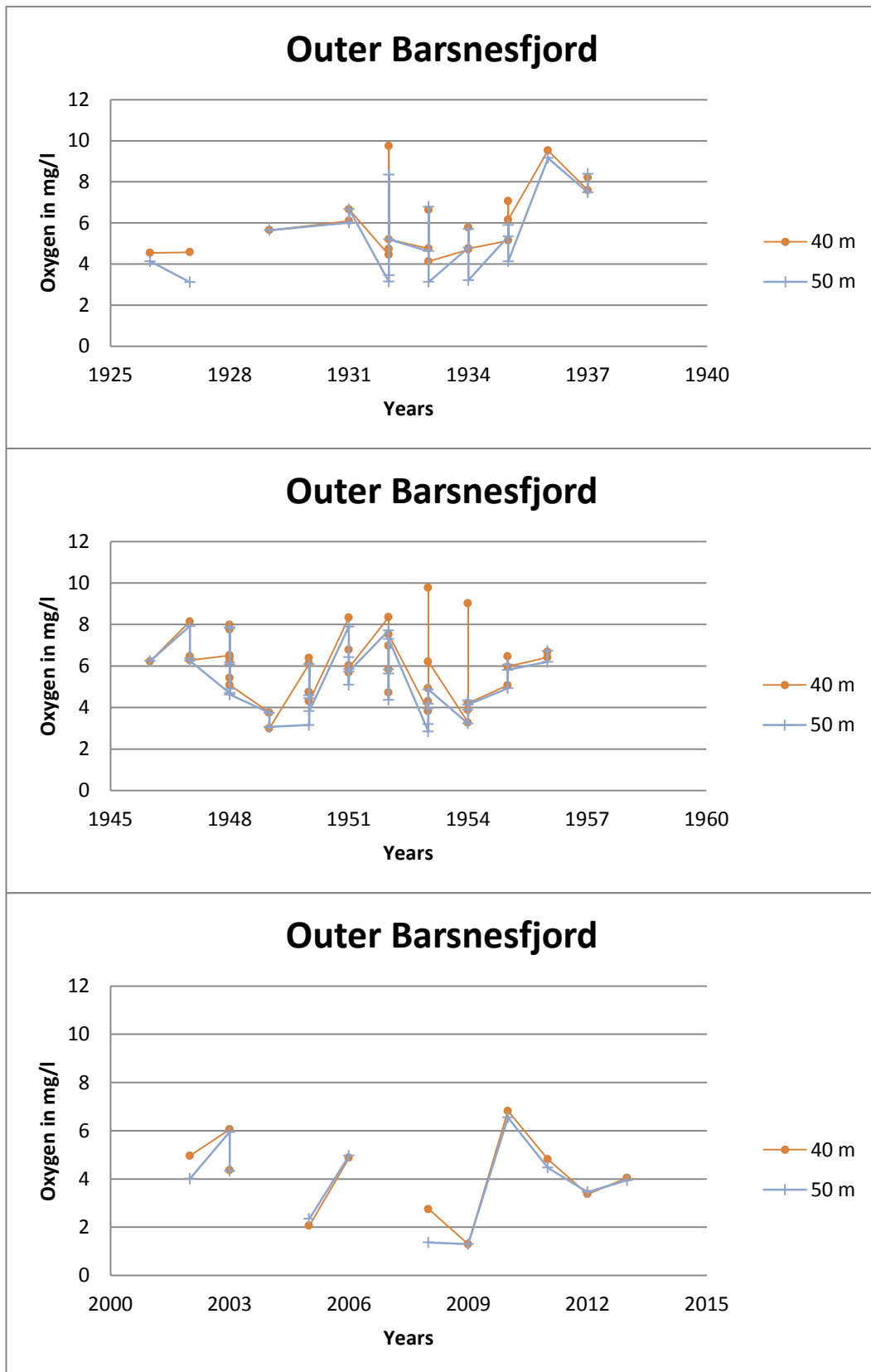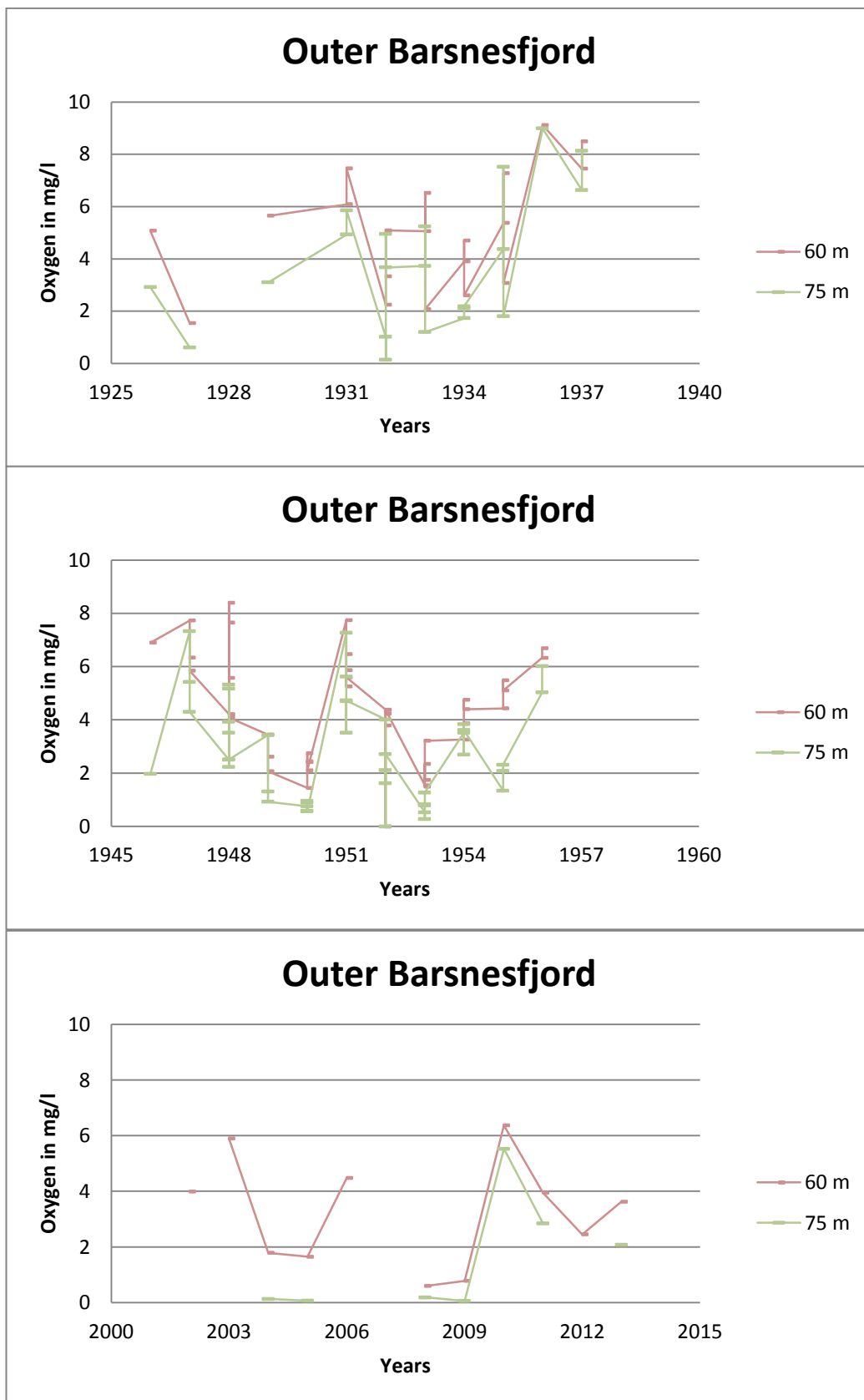
In Figure 31 the oxygen values of the Barsnesfjord from 1916-1937, 1946-1956 and 2002-2013 in the depths of 20 and 30 m are depicted. The first period and the second period have inflows every year, while the third period only has inflows every 3-4 years, namely in 2003, 2006, 2010 and 2013. Since the oxygen values in 2006 and 2008 are almost the same, it can be concluded that there has been an inflow in 2007 to compensate a yearly oxygen consumption of 0.5 mg/l to 1 mg/l. In the first two periods the values vary between 4 mg/l and 10 mg/l in both depths. In the last period, two alarming "killing events" happened in the 30 m layer, reaching values around 2 mg/l, namely in 2005 and 2009. The record shows that this low values at the 30 m depth have never been reached before and it is assumed, that these critical values had a great impact on the organism of the fjord that are living at these depth. The low levels in 2009 could for instance be related to the migration of the Norway lobster from deeper to shallower parts (Torbjørn Dale, 2014, *personal* communication).

In Figure 32 the oxygen values of the Barsnesfjord from the three periods in the depths of 40 and 50 m are depicted. The first period and the second period have inflows every year, except in 1927. The third period only has inflows every 3-4 years, namely in 2003 and 2006, 2010 and 2013.

Figure 33 shows the oxygen values in the depths of 60 and 75m. The first period has inflows every year. In this depth changes in the inflow years of the second period can be seen. Whereas in all other depths of the second period inflows occurred annually, in these depths the inflows occurred every 1-3 years, namely in 1947, 1948, 1951, 1954, 1955 and 1956. The third period has inflows every 3-4 years, namely in 2003, 2006, 2010 and 2013. The depths of 40-75 m represent the deep basin water, which is not influenced by the atmosphere, but only by the deep water renewal. It is noticeable, that 2009 was a year with extreme low oxygen concentrations in the deep water, with values between 0.06 mg/l in 75 m depth and 1.74 mg/l in 30 m depth. This probably caused many organisms to die or to flee to shallower depths that still contained more oxygen.

Table 2: Inflow rates of the tree periods in the depths 40, 50, 60 and 75 m. The inflow rate is calculated by dividing the years of the different periods with the number of inflows

Depths in m	Inflow rate Period 1	Inflow rate Period 2	Inflow rate Period 3
40	every 1.6 years	every 1.1 year	every 3 years
50	every 1.6 years	every 1.1 year	every 3 years
60	every 1.6 years	every 1.6 years	every 3 years
75	every 1.6 years	every 1.6 years	every 3 years

Table 2 visualizes the change in inflow year frequency. In period one and two the inflows occur approximately every year or every second year, whereas the inflow rate in period three is only every third year. The frequency of inflows in the two first periods is double compared to the third period.

4.2 Hydrographical results of the Sogndalsfjord

The Sogndalsfjord in Western Norway is a north-western directed tributary of the 204 km long and maximum 1308 m deep Sognefjord, which is connected to the open sea. The Barsnesfjord is a tributary of the Sogndalsfjord and thus also connected over the Sognefjord to the open sea (Figure 2).
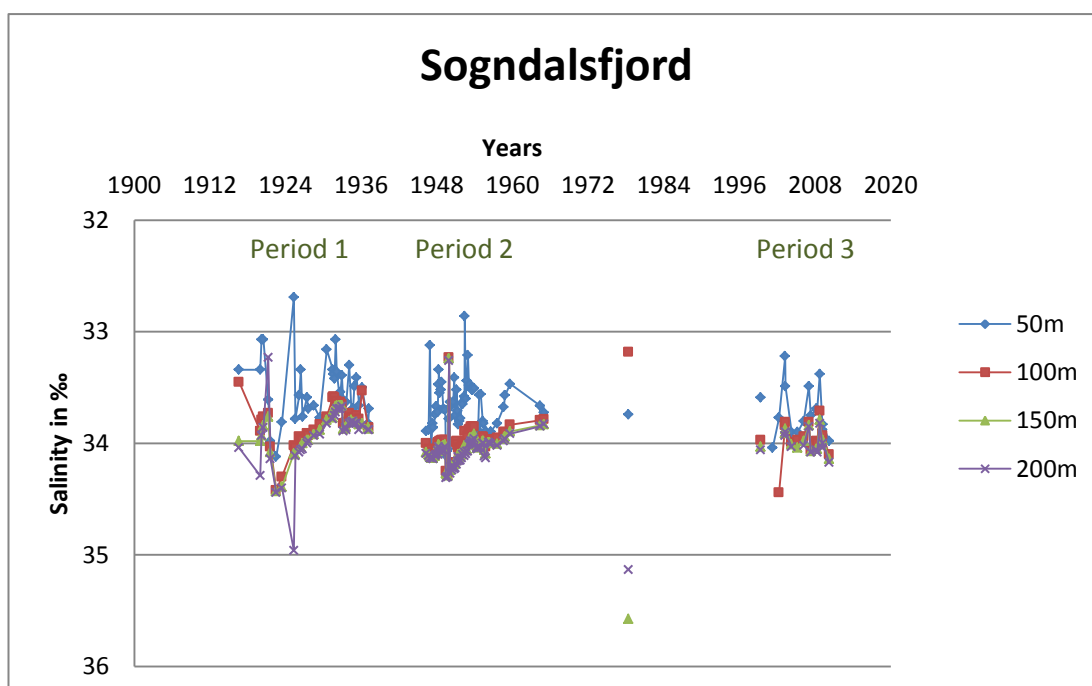
4.2.1 Salinity

Figure 34: Sogndalsfjord, whole dataset for salinity measurements in ‰ from 1916-2010, all depths

Figure 34 depicts the salinity of the Sogndalsfjord at water depths of 50, 100, 150, 200 and 250 m. The x-axis shows the year of sampling, the y-axis shows the salinity in ‰. The graph can be divided into three periods, as done in the graphs of the Barsnesfjord. The first segment starts in 1916 and ends in 1937. The salinity below 100 m depth fluctuates between 33.5‰ and 34‰. In 1925 a high salinity spike, almost reaching 35‰ at 200 m water depth, can be depicted. Also the measurements in 1923 show extraordinary high salinity values at depths from 100 to 200 m, namely around 34.5‰. At 50 m water depth, the salinity ranges mainly between 33‰ and 34‰, with one low salinity spike with 32.7‰ in 1925. From 1946 till 1965 the salinity below 100 m depth fluctuates between 33.8‰ and 34.3‰. In 1950 the measurements of the depths 100-200 m, which was taken in February, have an extremely low salinity around 33.25‰ in all three depths. At 50 m water depth, the salinities range like in the first period between 33‰ and 34‰, with one small spike in 1952 with a salinity of 32.86‰. The values of 1978 contain the lowest salinity value for the 100 m depth with 33.18‰. In the last segment from 1999-2011 the salinity values follow a "normal" trend again.

In the depths from 100 to 250 m the salinities range around 34‰, with one spike in 2002 with 34.44‰. At the 50 m depth the values fluctuate between 32.2‰ and 34‰. The decrease in salinity below 50 m in the Barsnesfjord in the period from 2000-2013 cannot be seen in the Sogndalsfjord, which leads to the thought, that the low salinity measurements in the Barsnesfjord might be correlated to a higher precipitation and a greater inflow of winter water from the Sogndalsfjord with water from the dams. Since the deep water inflow from the Sogndalsfjord in the Barsnesfjord is from depths shallower than 50 m, it would be necessary to look closer at these depths.

4.2.2 Temperature
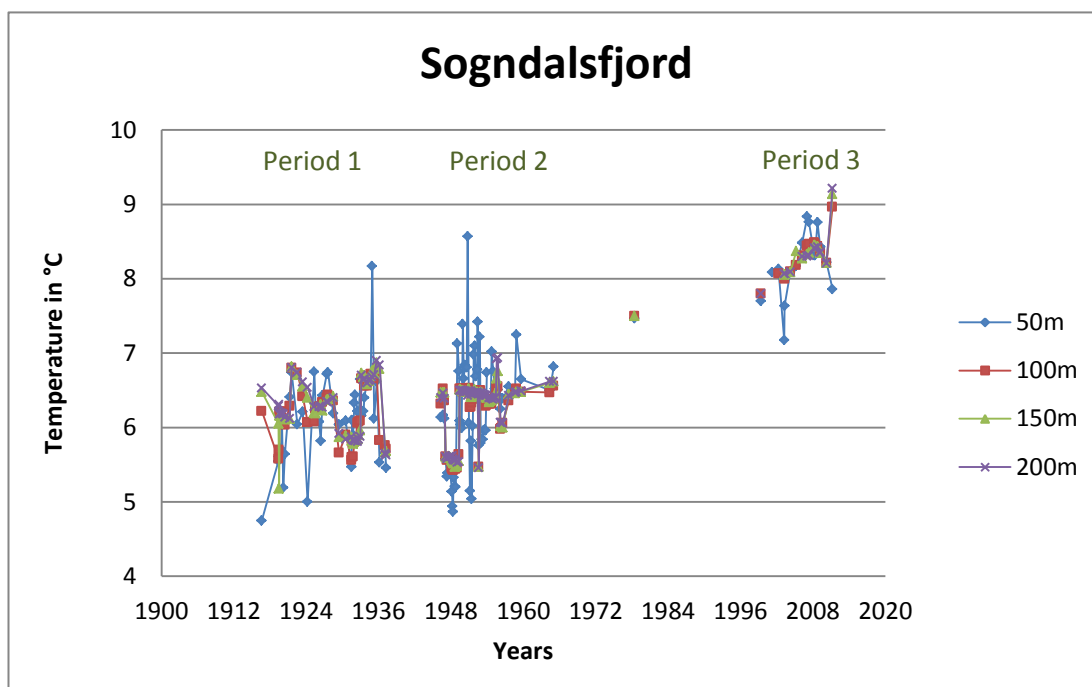
Figure 35: Sogndalsfjord, whole dataset for Temperature measurements in °C from 1916-2011, all depths

Figure 35 depicts the temperature of the Sogndalsfjord water column at water depths of 50, 100, 150, 200 and 250 m over. The x-axis shows the year of sampling, the y-axis shows the temperature in degrees Celsius (°C). The graph can be divided into three periods as in the salinity graph. The first segment starts in 1916 and ends in 1937. The water temperature below 100 m depth fluctuates between 5° and 7°C. At 50 m water depth, the temperatures range from 4.75° to 6.75°C with one spike at 8.17°C in January 1935. Within this time period the lowest temperatures between 5°C and 6°C were measured at all depths. From 1946 till 1965 the water temperature below 100 m depth fluctuates between 5.5° and 6.5°C. At 50 m water depth, the temperatures range from 4.87° to 7.42°C with one spike at 8.57°C in December 1950. In 1990 and 1991 the values of all depths range between 7° and 8°C. In the last segment from 1999-2011 the temperatures are the highest since the beginning of the record, fluctuating between 7.7° and 9.2°C in the depths from 100-250 m. Only one value in the 50 m depth reaches a slightly lower temperature of 7.2°C in 2003. A clear and strong rising trend in the temperatures of the Sogndalsfjord in the basin water can be determined.

4.2.3 Oxygen
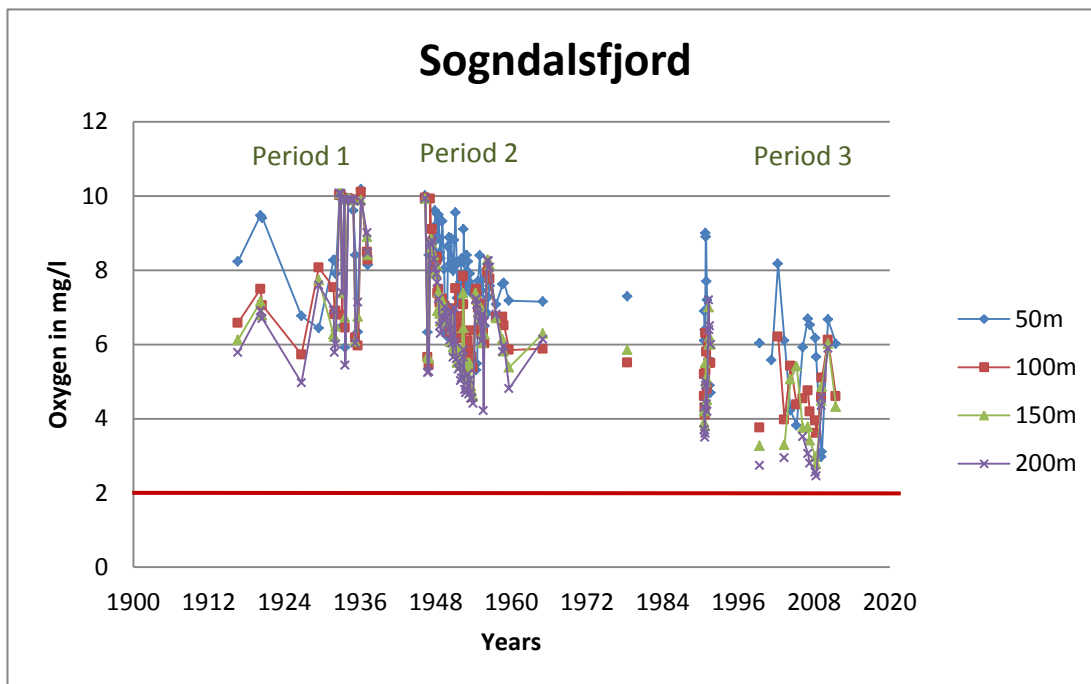
Figure 36: Sogndalsfjord, whole dataset for oxygen measurements in mg/l from 1916-2010, all depths. The red line at 2 mg/l illustrates the critical oxygen level.

Figure 36 shows the oxygen concentrations at the water depths 50, 100, 150, 200, and 250 m. The x-axis shows the calendar years from 1916 to 2011, while the y-axis indicates the oxygen concentration of the water samples in mg/l. The first segment starts in 1916 and ends in 1937. The oxygen concentrations fluctuate between 5 mg/l and 10 mg/l. In this part periods of the highest oxygen concentrations below 100 m water depth can be found. Such high oxygen concentrations in the deep basin water are connected with water exchange events. In the second period from 1946 till 1965 an apparent decrease in oxygen can be seen. From 1946 till approximately 1951 the concentrations were still quite high with values around 5 mg/l to 10 mg/l, but never reaching below 4 mg/l. From 1951-1965 the oxygen concentrations dropped, now ranging between 4 mg/l and 8 mg/l. In 1990 and 1991 the depths from 100 to 250 m hold the values ranging between 3.5 mg/l and 7.2 mg/l. Only the 50 m depth still has higher oxygen concentrations up to 9 mg/l. In the last segment from 1999-2011 the concentrations are the lowest since the beginning of the record, fluctuating between 2.46 mg/l and 6.21 mg/l in the depths from 100-250 m. Only one value in the depth of 50 m reaches 8.17 mg/l, namely in 2002, whereas other oxygen concentrations at this depth only range around 6 mg/l.

It can be reasoned, that a there is a clear and strong decreasing trend in the Sogndalsfjord, with oxygen concentrations nearly reaching the critical oxygen value of 2 mg/l. An extrapolation of this trend might suggest that the deepest parts in the Sogndalsfjord might experience values less than the critical level of 2 mg/l in near future.

4.2.4 Comparison Oxygen- Temperature in the Sogndalsfjord
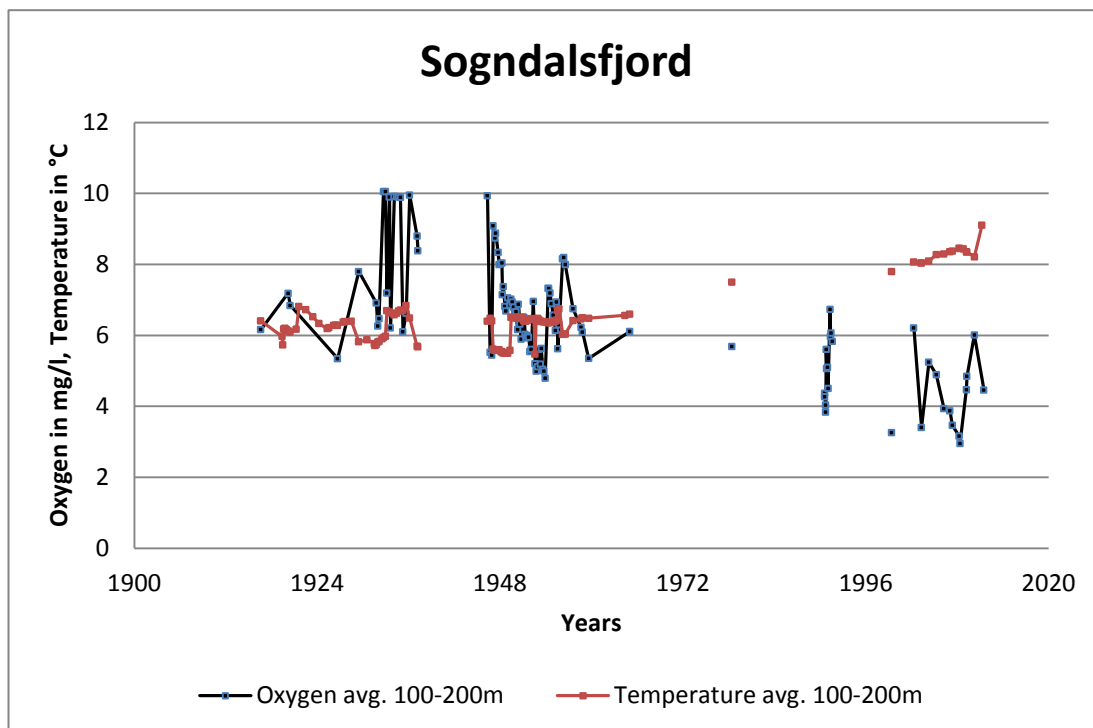
Figure 37: Sogndalsfjord, whole dataset for Oxygen measurements in mg/l in black and temperature measurements in °C in red from 1916-2011, average for the deeper depths 100, 150 and 200 m. An overall increase in temperature and an overall decrease in oxygen can be seen.

Figure 37 shows oxygen and temperature values of the Sogndalsfjord from 1916-2011. To compare both parameters better, the surface influenced depth of 50 m was left out and only the averages of 100, 150 and 200 m were calculated. Temperature and oxygen have an inverse correlation, since colder water can hold more oxygen than warm water and due to the additionally increased respiration in warmer water, which leads to a higher oxygen consumption. In the first two periods from 1916-1937 and 1946-1965 the oxygen and temperature values fluctuate within a similar range. Oxygen values lie between 5 mg/l and 10 mg/l, temperature values between 5.5°C and 6.5°C. Starting in 1990, the temperature reaches values between 7°C and 8°C, while oxygen values are missing.

In 1990 and 1991 oxygen values between 4 mg/l and 7 mg/l can be seen, here temperature values are missing. From 2002-2011 measurements for both parameters are available and show a clear separation of temperature and oxygen. While temperature increases up to a range between 8°C to 9°C, the oxygen values decrease accordingly to values ranging between 3 mg/l and 6 mg/l.

4.3 Hydrographical results of the Nordic Seas

4.3.1 Oxygen
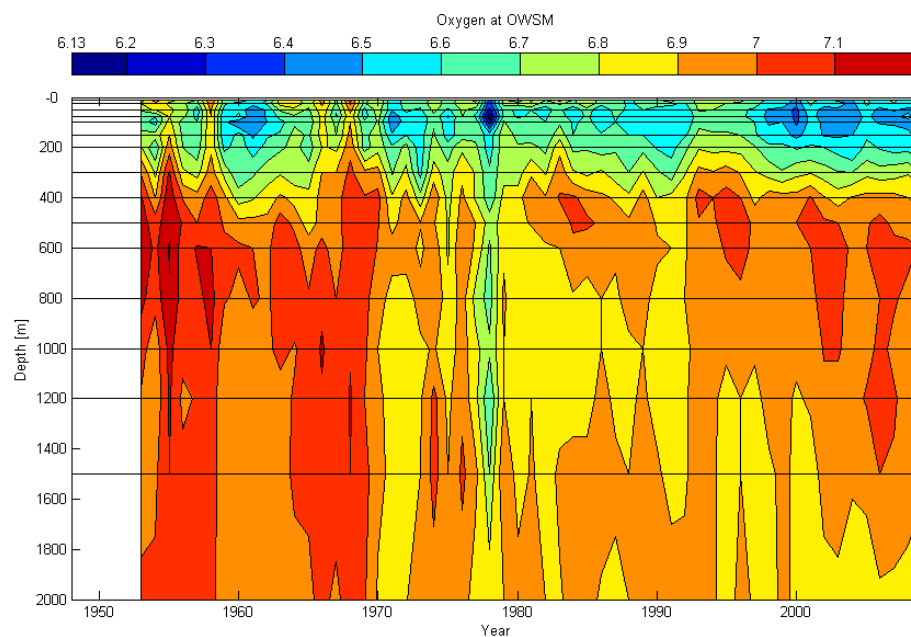
Figure 38: Oxygen concentrations in mg/l of the Norwegian Sea. Measured at "Station M" between 1953 and 2011 (http://www.eurosites.info/stationm.php, 2014). The x-axis shows the calendar years. The y-axis indicates water depth from 0 to 2000m. Red colour indicates elevated oxygen levels, blue colour indicates decreased oxygen.

The values of the oxygen concentration measurements from "Station Mike" (http://www.eurosites.info/stationm.php) are shown in Figure 38. The x-axis shows the years when the measurements were taken, namely 1953-2011 and the y-axis the depth in meter reaching from 0-2000 m. The colour gradient is used to show the oxygen concentrations. Red and orange is used for the highest oxygen concentrations of 6.9 to 7.3 mg/l, yellow and green stand for medium concentrations from 6.6 to 6.9 mg/l and the blue colour stands for lower oxygen concentrations of 6.13 to 6.6 mg/l.

Lower oxygen concentrations with values from 6.13 to 6.9 mg/l can be found at the surface and down to approximately 300m depth. The highest oxygen concentrations of 7 mg/l and higher can be found in the years 1953-1958. These high values even reach the 200 m depth. The whole water column seems to have high oxygen concentrations. Even the first 200 m have concentrations around 6.6 and 6.9 mg/l, which is high comparing it with values from the following years in these depths. The oxygen concentrations start to drop in 1958 throughout the whole water column. The oxygen concentrations in the surface waters dropped to 6.5 mg/l and between 800 m and 2000 m water depth they dropped to 6.9 mg/l. In the following ten years the oxygen concentrations in the deep water rose up to 7.1 mg/l, until 1970, when oxygen concentrations dropped to 6.8 mg/l.

This oxygen reduction is the beginning of the "Great Salinity Anomaly", which entered the Norwegian Sea during the years of 1978/79. This anomaly led to the strongest oxygen reduction in all water depths since the beginning of the record, with oxygen concentrations in the surface water of 6.13 mg/l, and oxygen concentrations of about 6.6 mg/l down to the depth of 1700 m and concentrations of 6.5 mg/l to depths of 1500 m. After this event, the oxygen started to increase again, but never reached the high levels from 1953 to 1958 so far. Since 1996 the surface layer has shown low oxygen concentrations from 6.4 to 6.6 mg/l, whereas the oxygen concentrations in the intermediate water layer increased. There are even some spots in the water column where concentrations of 7 mg/l were reached. The concentrations of large parts of the deeper water decreased to 6.8 mg/l.

4.3.2 Temperature
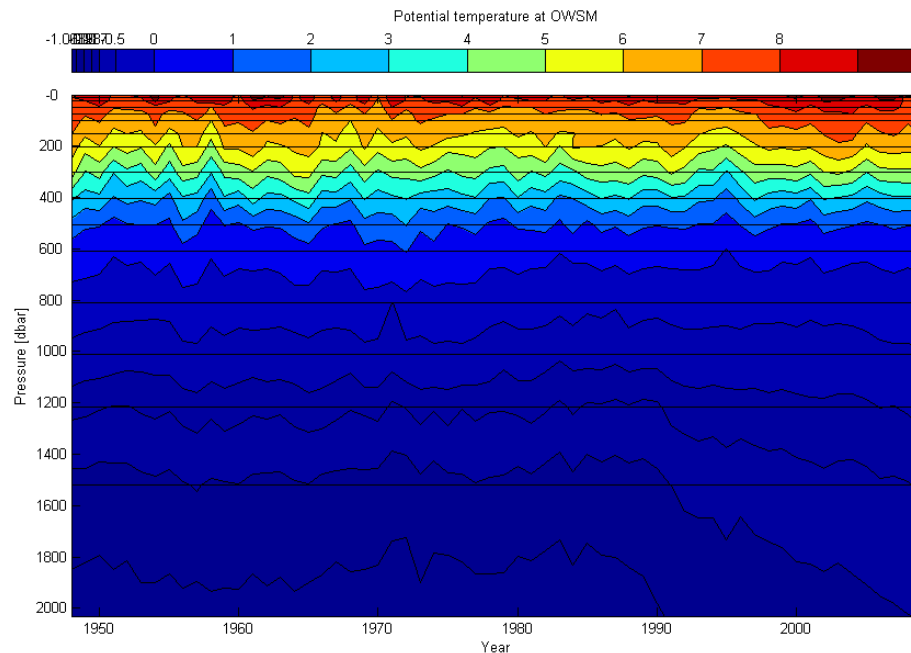
Figure 39: Potential water temperature of the Norwegian Sea. Measured at "Station M" between 1948 and 2011 (http://www.eurosites.info/stationm.php, 2014). The y-axis indicates water pressure, corresponding to water depth (0-2000 dbar corresponding to 0-2000 m water depth). The "potential temperature" refers to the water temperature in °C calculated for a standard reference pressure at the indicated depth.

Figure 39 shows the potential temperature at the "Station Mike". The x-axis shows the years from 1948-2011 and the y-axis indicates the water pressure in dbar. The pressure in dbar and the depth in meters are approximately equal, so the pressure of 1 dbar in the ocean correspondents with about 1 m depth. The potential temperature scale refers to the water temperature (in °C) calculated for a standard reference pressure at the indicated depth. The blue colour shows the coldest water temperatures, which occur in the deep parts of the ocean, and the red colour represents the warmest water temperatures, which are occurring at the surface. The highest temperatures can be found at the surface due to the North Atlantic Current, which represents the northwards continuation of the Gulfstream. Since about 1985, the temperatures of the whole water body have increased in the Norwegian Sea. The warming trend began at 2000 meters depth, spread to 1500 m depth, and then to 1200 m. This warming is of great significance, taking into account that the water layers that are being warmed up are at depths of 1000-2000 meter. Since the ocean water has an enormous thermal heat capacity, this means that the heating process is very slow.

4.3.3 Salinity
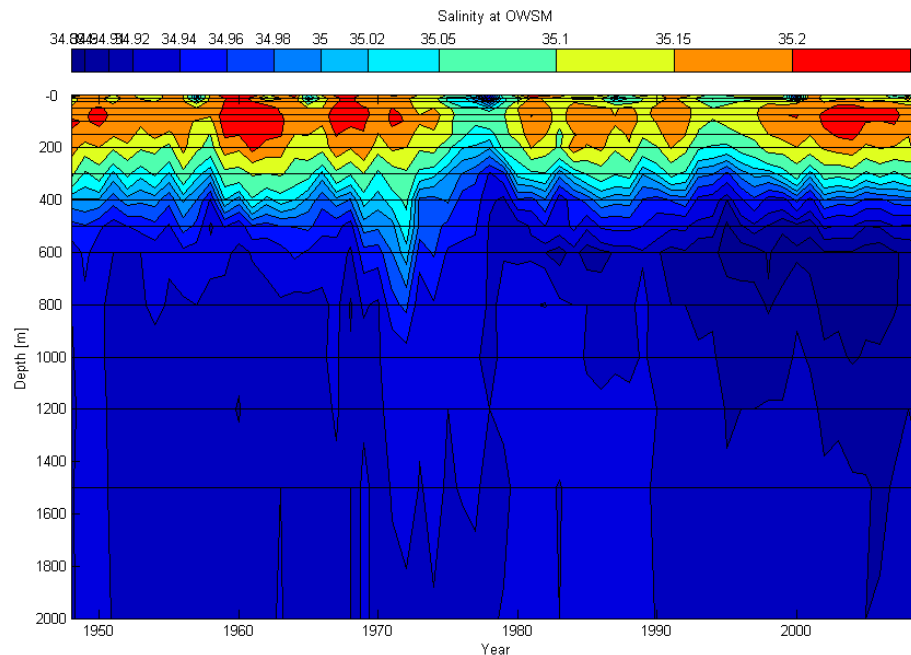
Figure 40: Salinity in ‰ of the Norwegian Sea. Measured at "Station M" between 1948 and 2011 (http://www.eurosites.info/stationm.php, 2014). The x-axis depicts calendar years. The y-axis shows water depth from 0 to 2000m. Red colour indicates increased salinities, blue colour indicates decreased salinities.

Figure 40 shows the salinity in ‰ of the Norwegian Sea measured at "Station M". The x-axis depicts the years from 1948 till 2011. The y-axis indicates water depth from 0 to 2000 m. The red and orange colours indicate higher salinities around 35.1 to 35.25‰; the blue colours indicate lower salinities around 34.8 to 35.1‰. The first 300 m of the ocean are made up of warm and salty Atlantic Ocean water. This water comes from the Gulf Stream and is called the Norwegian Atlantic Current. From about 1960 to 1969 there was a period of warm and salty water in the upper water layers. In 1969 was an abrupt shift to a period with low salinity concentrations due to large amounts of fresh water. This powerful climate signal in the Atlantic Ocean was called the "Great Salt Anomaly" and lasted until 1982. It most likely started in the Greenland Sea at the end of the 1960s, reached Station M about ten years later, after following a cyclical path in the Atlantic Ocean (Cicero, 2014). There are several ideas about the reason for the "Great Salt Anomaly". The low concentrations in salinity that were observed successively around the North Atlantic could be due to advection of a fresh water anomaly along the main ocean currents.

Serreze & Barry (2005) suggested that more sea ice was transported by strong northerly winds into the Greenland Sea through the Fram Strait. When the ice melted, an increasing fresh water influx occurred, which resulted in a decrease of salinity concentrations. Since 2000, the salinities at the surface layer are high again, which could be connected to a change in the major air circulation cells in the North Atlantic (Cicero, 2014).

4.4 NAO Winter Index
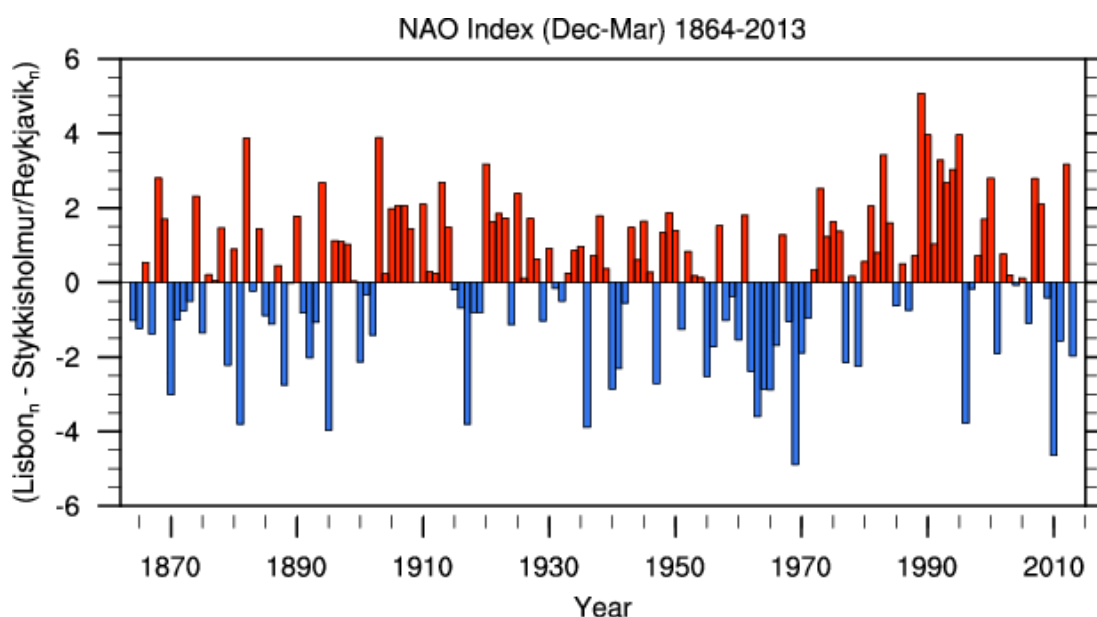
Figure 41: Winter (December through March) index of the NAO based on the difference of normalized sea level pressure (SLP) between Lisbon, Portugal and Stykkisholmur/Reykjavik, Iceland since 1864. The SLP values at each station were normalized by removing the long-term standard deviation. Both the long-term means and standard deviations are based on the period 1864-1983. Normalization is used to avoid the series being dominated by the greater variability of the northern station. (Climate Data Guide; A. Phillips, 2014)

Figure 41 shows the winter (December-March) station-based NAO index. It is based on the difference of normalized sea level pressure, short SLP, between Lisbon, Portugal and Stykkisholmur/Reykjavik, Iceland (Climate Data Guide, 2014). The data is from 1864 till 2013. The x-axis shows the time scale in years, while the y-axis shows the NAO winter index in its positive phases in red and its negative phases in blue. This graph focuses on the Northern Hemisphere winter months, since the influence of the NAO on surface temperature and precipitation is the greatest at this time of year (Hurrell & Deser, 2009). The North Atlantic Oscillation is the leading pattern of weather and climate variability over the Northern Hemisphere.

The NAO changes from a positive to a negative phase, and thereby produce large changes in air temperature, winds and precipitation over the Atlantic and the nearby continents. The oceans heat content, gyre circulations, the depth of the mixed layer, salinity and sea ice cover are also affected by the North Atlantic Oscillation. A positive NAO index is associated with stronger-than-average westerlies, resulting in more and stronger winter storms crossing the Atlantic Ocean on a more northerly track. This leads to warm and wet winters in north-western Europe and to cold and dry winters in Mediterranean region. The negative NAO index phase is associated with fewer and weaker winter storms, which cross on a direction from west to east. This leads to wetter conditions in the Mediterranean and cold and dry air in Northern Europe. The graph shows several periods of negative or positive phases, when anomalous circulation patterns occur over many winters in a row. From 1900-1930 was a sequence of positive NAO winter index, which led to warmer than normal winter temperatures over most of Europe (Hurrell, 1995). From the 1940s to the early 1070s the NAO index had a negative trend, with lower than normal winter temperatures over Europe. Since 1980 strongly positive NAO index values can be measured, with the most positive phase recorded in 1989. During the winters 2009 and 2010, the NAO winter index is quite negative, resulting in cold winters in Middle and Northern Europe. This negative trend did not last long, for in the winter of 2011 and 2012 a positive NAO winter index can be seen again, which resulted in a mild winter in Middle and Northern Europe.

5. Discussion

To be able to make a trustworthy discussion, it needs to be kept in mind, that there might be small measuring inaccuracies that could have occurred due to different methods used over time. Since these data covers a time period of 100 years, there were changes in the methodology, for the measuring technology changed and improved over time. All methods that were used are decent and give respectable values, but they still might vary from each other. Another factor that always needs to be kept in mind is the fact, that for the last period from 2002-2013 there are only autumn values available, whereas the previous values were taken throughout the year and also include several measurements in one year. To be able to exclude this possible error, Figure 42 illustrates the differences between the temperature values that were taken throughout the year (Figure 42a) and those values that were only taken in autumn, namely August and September (Figure 42b). The depths are 40, 50, 60 and 75 m. The overall increasing trend of the temperatures is unmistakably visible in both figures. Only some of the spikes that occur in the measurements throughout the year are missing in the autumn values. It thus can be concluded that a possible deviation from the "real trend", due to too many measurements throughout the year, can be suspended for the most part.
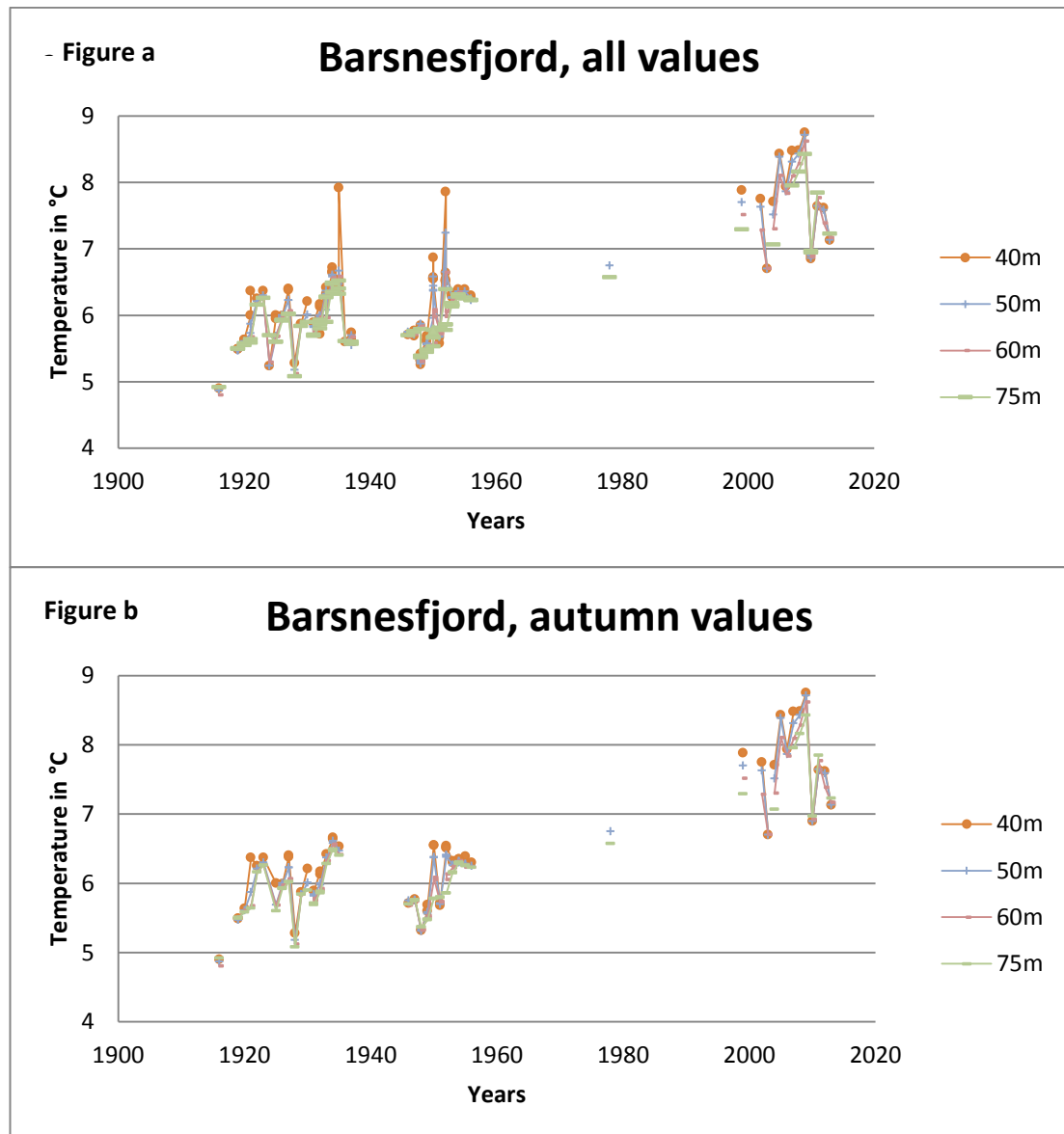
Figure 42: Temperature values of the Barsnesfjord from 1916 to 2013 with the depths of 40, 50, 60 and 75 m. Figure 42a shows all measuered values throughout the whole year. Figure 42b shows only the autumn values, namely August and September.

5.1 Water temperature variations

Within all measured depths of the Barsnesfjord an increase in the water temperature, happening during the time period between 1956 and 1990, can be indicated (Figure 21). The water temperatures of the basin water deeper than 20 m are approximately 1.7°C higher in the third period compared to the temperature values from the first period of 1916-1937 (Table 3). The temperature differences between the first and the second period are very small, showing that the first and second periods hold fairly stable water temperatures at all depths.

Since there are no measurements between 1956 and 1978, it can only be guessed when the increase in water temperature started and how fast and acute it occurred. The depths from 0 to 10 m are strongly influenced by the atmosphere. This can be seen in the high increase values of around 4°C. This strong increase can be easily explained. The values of the last period are only taken in August and September, when the water has reached its highest surface temperature due to the strong summer irradiation. Since the first two periods show measurements throughout the year they also include the cold winter temperatures, which decrease the average temperature of these depths. At greater depths, where the atmosphere does not have such a strong influence on the water temperature, the real temperature increase can be seen, namely an increase between 1.6° and 1.75°C. This reflects a temperature increase in the water flowing into the basin from the Sogndalsfjord and Sognefjord. The inflow from the Sogndalsfjord into the Barsnesfjord happens in wintertime. The inflowing water comes from the depths of 7-20 m of the Sogndalsfjord.

Table 3: Average water temperature values of the three main periods. The first column depicts the depths in meter from 0 to 75 m. The second column shows the average water temperature in the first period from 1916-1937 from every depth. The third column depicts the second period from 1946-1956 and the forth column shows the third period from 2002-2013. The last column represents the increase in temperature from the first to the third period in °C.

Depths	1.) 1916-1937	2). 1946-1956	3.) 2002-2013	1. and 3. period
	Temperature in °C	Temperature in °C	Temperature in °C	Increase in °C
0	9,01	9,76	13,15	4,14
5	10,30	11,01	14,30	4,00
10	8,24	9,02	11,41	3,17
20	6,37	6,62	7,97	1,60
30	6,14	6,13	7,77	1,63
40	6,04	6,09	7,72	1,68
50	5,92	6,02	7,67	1,75
60	5,89	5,91	7,56	1,68
75	5,86	5,86	7,57	1,72

5.1.1 Influences of the Nordic Seas surface water warming on the Barsnesfjord

An increase in the water temperature of the basin water of the Barsnesfjord occurred during the time period between 1965 and 1990, as well as in the water masses of the Sogndalsfjord, where the temperature increase started sometime between 1965 and 1978 (Figure 43).

Temperature Basinwater Sogndalsfjord- Barsnesfjord
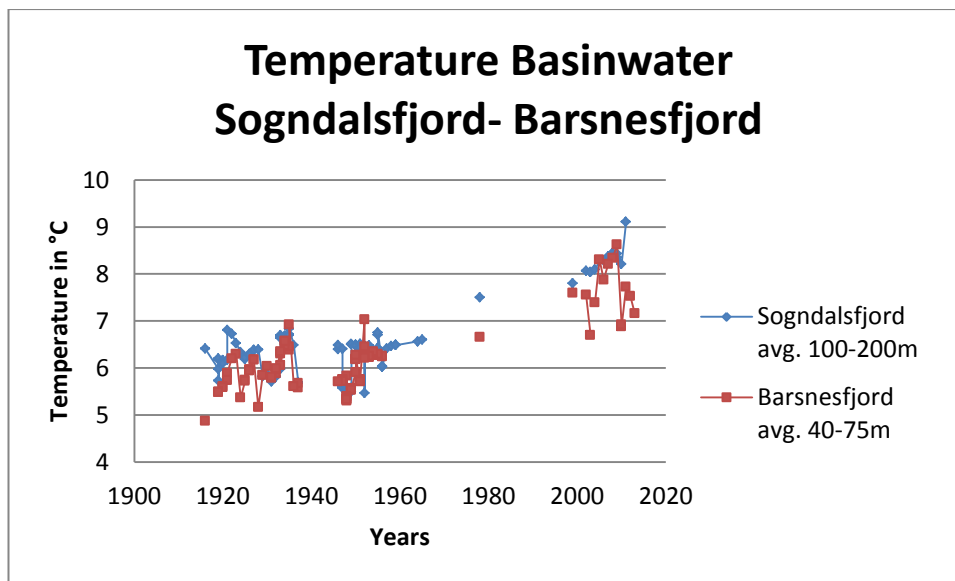
Figure 43: Comparison of the Temperature in °C in the Basin waters of the Sogndalsfjord and the Barsnesfjord. The Sogndalsfjord is represented by the blue line, showing the depths 100, 150 and 200 m. The Barsnesfjord is represented by the red line and shows the depths 40, 50, 60, 75 m.

This significant temperature increase cannot be detected in the deep water layers of the Nordic Seas data set before 1985 (Figure 39). Since the surface water masses that are measured at "Station Mike" influence the basin water of the Sogndalsfjord and the Barsnesfjord, it can be suggested that the warming of the Barsnesfjord and the Sogndalsfjord after 1985 could be influenced by the increasing temperatures of the surface waters of the Nordic Seas. To be able to explain the increasing water temperatures of both fjords between 1965 and 1990 a closer look at the temperature anomalies at "Station Mike" (Figure 44) might be helpful. The temperature anomalies measured at "Station M" depict the deviation from a long time average of the temperature. A positive anomaly is shown in a light green to red and indicates that the observed temperature is warmer than the long-term value. A negative anomaly, shown in blue colours, indicates colder than average temperatures.

When analyzing the temperature anomalies between 1960 and 1970, an overall increase in the surface water temperature of the Nordic Seas surface waters can be seen. This increase could be related to the temperature increase in the Sogndalsfjord and the Barsnesfjord, which happened at the same time.
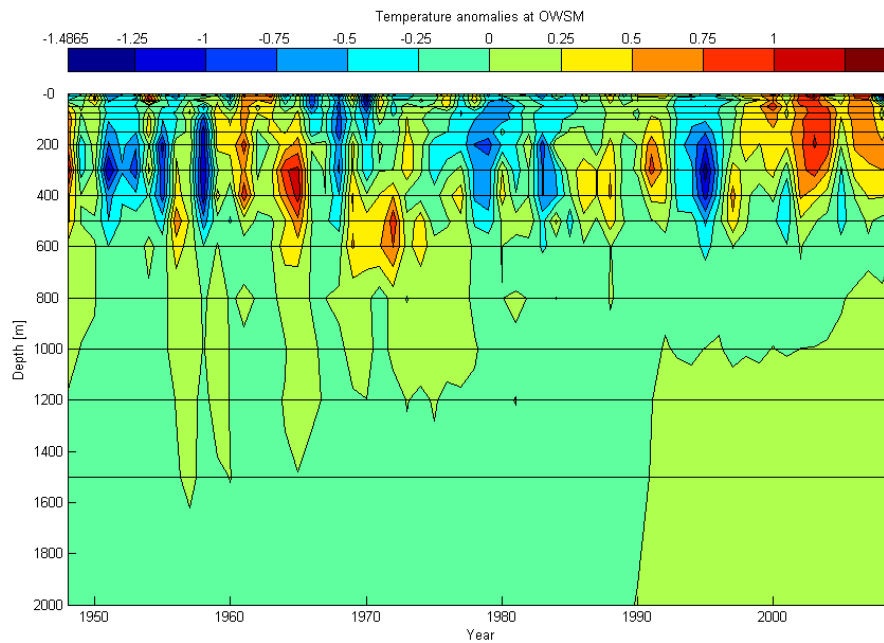
Figure 44: Temperature anomalies at the "Station Mike" (http://www.eurosites.info/stationm/data.php). Temperature anomalies indicate a departure from a long-term average value. A positive anomaly indicated by light green to red, shows that the observed temperature is warmer than the long-term value. A negative anomaly, which is represented by blue colours indicates a colder than average temperature.

The question that arises is what caused the surface water increase of the Nordic Seas. One possible explanation could be an influence from the atmosphere, caused by the North Atlantic Oscillation (NAO). From 1900 to 1930 a sequence of positive NAO winter index values could be seen, which led to warmer than normal winter temperatures (Figure 41). From the 1940s to 1965 the NAO index shows a period of more frequent negative NAO winter index values, with colder than normal winter temperatures over Europe. Since 1965, the values of the NAO winter index are mainly positive, with a positive trend until 2009. The greatest positive NAO winter index values are reached between 1990 and 1995. This strong shift from strong negative to strong positive NAO winter index values between 1965 and 1990/1995 could be responsible for the temperature increase in the surface water layer of the Nordic Seas and accordingly in the Sogndalsfjord and Barsnesfjord water masses

starting in the period between 1965 and 1999. Due to increasingly positive NAO conditions, warm and moist southerly airflows along the North Atlantic occur. They are responsible for driving a warmer and stronger flow of Atlantic water northwards to the Barents Sea and into the Arctic Ocean, which can be observed since the 1960s (Dickson & Østerhus, 2007). This connection between the NAO winter index and the inflowing Arctic water into the northern Greenland Sea are depicted in Figure 45. Figure 45a shows the temperature of the Arctic waters that are entering the northern Greenland Sea with an increase of approximately 1.5°C in the period from 1965-1999. Figure 45b depicts the annual, filtered NAO winter index. A connection between the NAO winter index and the increasing temperatures of the Nordic Seas surface waters can be drawn.
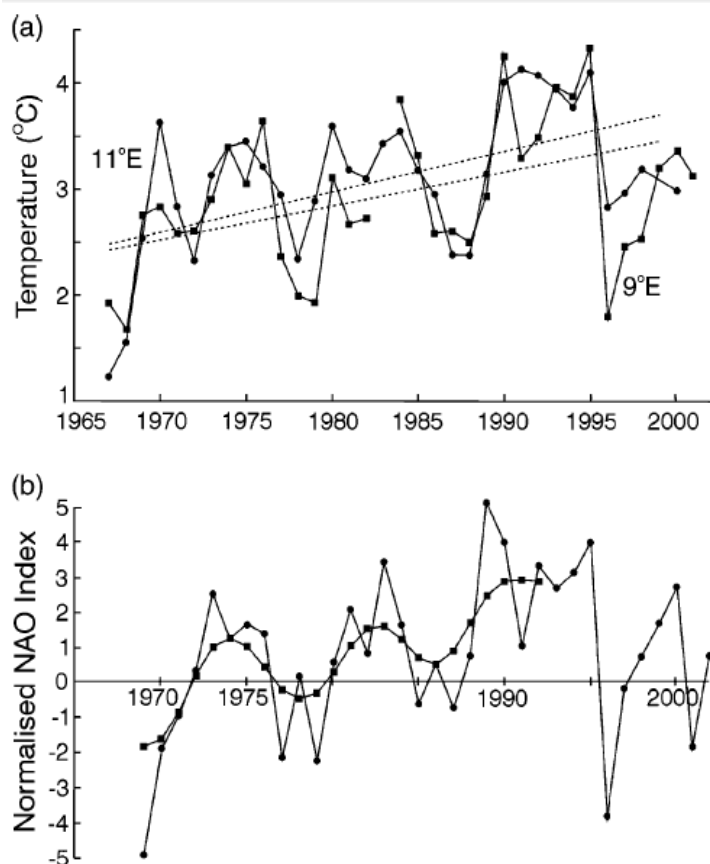

Figure 45: Comparison between the NAO winter index and the Fram Strait surface water temperatures: 45a Mean water temperatures at 500 m water depth in August-September at 9°E and 11°E, i.e. along the Sørkapp Section; 45b The normalized winter NAO index (yearly and filtered). Figure adapted from Dickson & Østerhus (2007).

Between 1968 and 1982 the Great Salinity Anomaly can be observed (Figure 40), which coincides with the increasing water temperatures of the Sogndalsfjord and the Barsnesfjord. Since the Great Salinity Anomaly also coincides with the most negative NAO winter index observations (Figure 41), a connection between them could be concluded. During the Great Salinity Anomaly more sea ice was transported by strong northerly winds into the Greenland Sea through the Fram Strait (Serreze & Barry, 2005). When the ice melted, a great fresh water influx occurred, which resulted in decreasing salinity and colder surface water masses in the Nordic Seas. With decreasing salinities and the accordingly decreasing water temperatures the North Atlantic thermohaline circulation was weakened (Timmermann et al., 1998). Thermohaline circulation describes the ocean water circulation pattern that is driven by density differences, which occur due to changes in salinity and temperature.

It is suggested that low salinities lead to a strengthening of the pressure differences between the Icelandic Low and the Azores High, which then leads to colder sea water temperatures. This strengthened pressure difference led to the negative phase of the NAO winter index that occurred during the Great Salinity Anomaly between 1968 and 1982 (Bader & Kunz, 2000). After 1980 the salinities at the surface layer of the Nordic Seas increase, strong positive NAO index values can be measured, with the most positive phase recorded in 1989. These factors might be responsible for the warming in the Sogndalsfjord and Barsnesfjord water column during the period 1965-1999.

5.1.2 Influence of the Nordic Seas deep water warming on the Barsnesfjord

The "Great Salinity Anomaly" in the years from 1968-1982 affected the deep water masses of the Nordic Seas. The anomaly is responsible for a slight decrease of the water temperatures of the deep water masses of the Nordic Seas. After the "Great Salinity Anomaly", around 1985, an increase trend in the water temperatures in the Nordic Seas can be detected, which was starting at a depth around 2000 m and continuously grew shallower to the depths of 1800 and 1200 m in the years 1990

and 1991 (Figure 39). This increase in deep water temperature could additionally be related to the increasing water temperatures in the Sogndalsfjord and the Barsnesfjord after 1985 (Figure 43). The question that arises is what caused the increase in temperature of the deep waters of the Nordic Seas. Østerhus and Gammelsrød (1999) argued that the warming trend of the deep waters of the Nordic Seas is caused by a reduced inflow of cold Greenland Sea water into the Norwegian Sea since 1985. The water masses of the Greenland Sea have become warmer, which accordingly led to a warming of the deeper water masses of the Norwegian Sea.
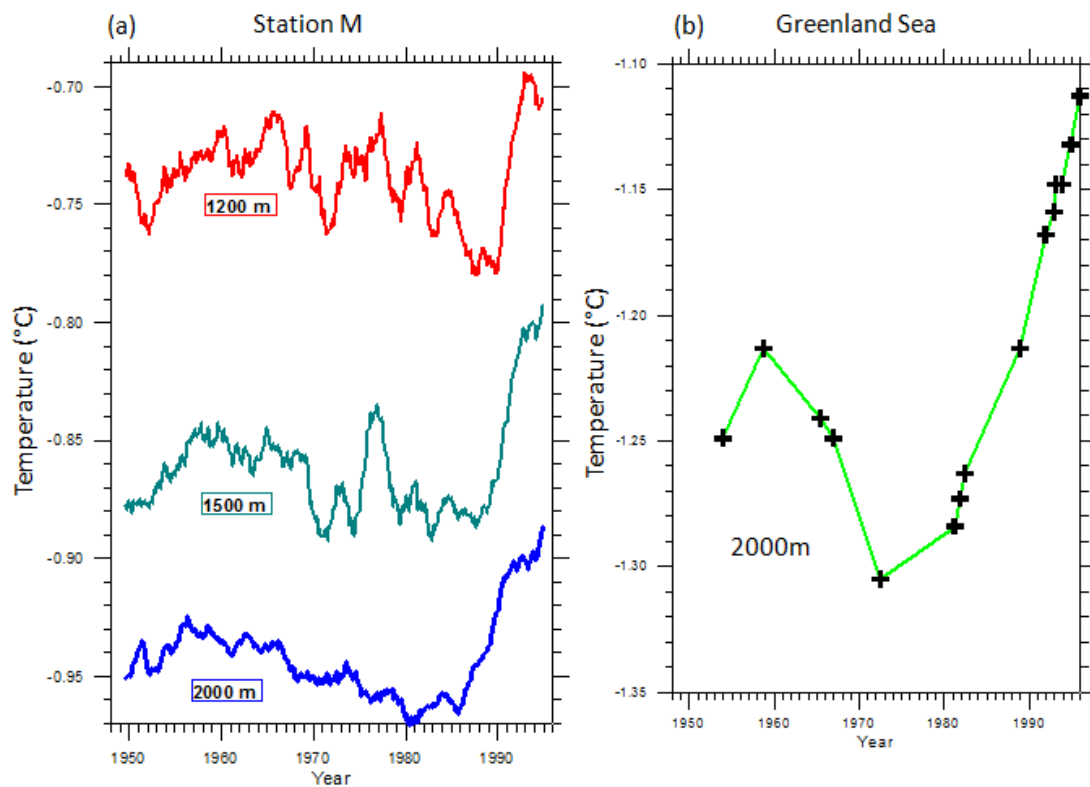
Figure 46: Temperature increase in the Nordic Seas deep waters: 46a Water temperature (in °C) taken at 1200, 1800 and 2000m water depth at the "Station M" between 1948 and 2000; 46b Water potential temperature (in °C) taken at 2000m water depth in the Greenland Sea between 1953 and 2000. The figure is adopted from Østerhus and Gammelsrød (1999).

Figure 46 shows the temperature increase in the Nordic Seas deep waters, taken at the depths of 1200, 1800 and 2000 m at the "Station M" between 1948 and 2000. Figure 46b depicts the potential water temperature taken at 2000 m water depth in the Greenland Sea in the years from 1953 to 2000.

The observed warming of the Greenland Sea at 2000 m starts around 1980. In the Nordic Seas the warming trend is first visible at 2000 m water depth in the year 1985, which is followed by a similar warming trend at 1800 and 1200 m water depth around 1990 and 1991 (Figure 39).

5.2 Oxygen Variations

The oxygen concentrations are highest in the upper layers and decrease with depth within the examined water bodies, namely the Barsnesfjord (Figure 26) and the Sogndalsfjord (Figure 36). The Nordic Seas on the other hand showed an opposite trend, with lower oxygen concentrations in the upper part and higher oxygen concentrations below 400 m (Figure 38). The reason for the high oxygen values in the upper layer in the Barsnesfjord and the Sogndalsfjord is due to a constant gas exchange with the atmosphere. Furthermore, the upper layer is the zone where photosynthesis is possible, which additionally leads to high oxygen values. At depths greater than the euphotic zone, oxygen concentrations continuously decrease due to respiration processes in the stagnant waters. The oxygen concentrations in the deep waters only increase when new water with higher oxygen concentrations is carried into the basin water of the fjords from the open ocean or another fjord.

Table 4 shows a decreasing trend in the oxygen concentrations at all depths. The table depicts the average oxygen concentrations of the three main periods of measurement. The first column shows the depths in meter from 0 to 75 m. The second column shows the average oxygen concentrations in the first period from 1916-1937 form every depth. The third column depicts the second period from 1946-1956 and the forth column shows the third period from 2002-2013. The last column represents the decrease in oxygen values from the first to the third period in %.

Table 4: Average oxygen concentrations of the three main periods in the Barsnesfjord. The first column depicts the depths in meter from 0 to 75m. The second column shows the average oxygen concentrations in the first period from 1916-1937 from every depth. The third column depicts the second period from 1946-1956 and the forth column shows the third period from 2002-2013. The last column represents the decrease in oxygen values from the first to the third period in %.

Depths	1.) 1916-1937	2). 1946-1956	3.) 2002-2013	1. and 3. period
In m	Oxygen in mg/l	Oxygen in mg/l	Oxygen in mg/l	Decrease in %
0	12,00		9,36	-22,03
5	10,44	10,84	9,17	-12,18
10	9,90	10,33	9,22	-6,83
20	7,94	7,77	6,38	-19,74
30	6,46	6,15	4,45	-31,09
40	6,12	5,94	4,13	-32,49
50	5,58	5,28	3,88	-30,47
60	5,19	4,35	3,31	-36,19
75	3,82	2,89	1,56	-59,21

The average decrease is strongest in the deeper parts from 30-75 m. In the depths of 30, 40 and 50 m the decrease in oxygen from the first to the third period lie between 30 and 32%. At 60 m with a decrease of 36% and at 75 m with a decrease of 59% the oxygen values dropped significantly. The decrease is not as high in the upper layers, which is due to the atmospheric exchange of oxygen with the upper water layers and the photosynthesis. But still there is a decrease in oxygen, which is caused by the fact that the water temperatures in the basin water of the Barsnesfjord have increased significantly over the years.

Marine water holds less free oxygen at warmer temperatures than at colder temperatures. With increasing temperatures, also the rate of metabolism in marine animals increases. The metabolic rate doubles with an increase in temperature of 10°C (Pearson, 2014). This means that with an overall increase of temperatures of approximately 1.7°C in the basin water (Table 3), the metabolism rate increased by 17%. Cellular enzymes are more active when the temperature increases, which leads to a greater oxygen consumption.

For this reason, the low oxygen concentrations in the Barsnesfjord during the last 10 years could be explained by the increasing water temperatures. This factor is probably also responsible for the reduction of the oxygen concentration that occurs at the same period in the Sogndalsfjord (Figure 36) and the Nordic Seas (Figure 38). In addition the Sogndalsfjord and the Nordic Seas also hold less oxygen, the supply of oxygen rich basin water decreased, causing the basin waters of the Barsnesfjord to become more often stagnant.

Not only the quality of the inflows changes, also the quantity grew smaller. In the basin water of the Barsnesfjord the same inflow pattern could be detected (Figure 31, 32, 33). In the first period from 1916-1937 and the second period from 1946-1956, inflows of new basin water occur every 1.1-1.6 years, whereas in the third period from 2002-2013 the inflows are very irregular and only occur every 3 years (Table 2). This shows that there are changes in the inflow regime from the first and second period to the third period. These changes can be explained by various factors.

The top 10 m are not influenced by the water renewal trough inflowing water from the Sogndalsfjord. The reason for the strong oxygen variations in the two first periods could be due to winter convection in the surface waters. Since there are measurements throughout the whole year, the temperatures and thereby the oxygen concentrations change accordingly. The high oxygen values are measured in the winter months, when the cold water can hold more oxygen. The last period only represents autumn values, when the water has reached its highest temperature. In this period the oxygen concentrations are not fluctuating as strong as in the first two periods and do not reach high oxygen values either. This is due to the fact that in this period no measurements exist that could indicate the winter convection.

In the deeper layers, starting approximately at 30 m water depth, the variations are connected to the changes in the inflowing regime. These changes could have occurred due to a density reduction of the inflowing deep waters, namely the Sogndalsfjord, the Sognefjord and the coastal current.

The inflowing water needs to have a higher density to be able to float over the sill and sink to the basin water of the fjord. The density of the inflowing water of the Sogndalsfjord is reduced due to an increase in temperature (Figure 35). A decrease in salinity could also be possible for the density reduction. It is possible, that a salinity reduction occurred in the first 50 m of the Sogndalsfjord, which represent the inflowing water. A proper conclusion about this cannot be drawn, since the available data start at a depth of 50 m. The data from 0, 5, 10, 20, 30 and 40 m in the Sogndalsfjord exist, but have not been worked up yet.

Another possible factor is the change in wind direction which is affected by the NAO winter index (Figure 41). From the 1940s to the early 1070s the NAO winter index had a negative trend, which results in fewer and weaker winter storms, which cross from west to east and bring cold and dry air to Northern Europe. Since 1980 strongly positive NAO index values can be measured, with the most positive phase recorded in 1989. Even though there was a negative NAO winter index in the years of 2009 and 2010, the negative trend did not last long. In the winter of 2011 and 2012 a positive NAO winter index can be seen again, which makes this in average a positive NAO winter index phase. This positive NAO winter index leads to south-westerly winds, which then result in more and stronger winter storms crossing the Atlantic Ocean and reaching Europe. A positive NAO will accumulate low density water along the coast with a deepening of the coastal wedge and thereby prevent the upwelling of dense deep water on the coast and the flowing in to the fjords (Torbjørn Dale, 2014, *personal* communication).

Another possible factor for the change in the inflow years is the freshwater outflow in wintertime, which occurs unnaturally due to the hydroelectric power production. Most of the big hydroelectric power plants using dammed water were installed by the 1970-1980s. This has lead to an increased freshwater flow in winter time and a reduction in summertime.

Another factor that might have strongly influenced the inflows is the building of the Loftesnesbridge in 1958. When the bridge was built, the sill was most probably filled up and thereby the sill depth was reduced to its present-day depth.

This infill might have generated a barrier for the inflowing water of the Sogndalsfjord into the Barsnesfjord. To be able to overcome the filled up sill, the inflowing water needs to have a greater density, which, as described earlier, is reduced in addition.

5.3 Salinity variations

The salinity values of the Barsnesfjord do not follow the same pattern as the oxygen and temperature values, which were showing the same changes as in the Sogndalsfjord and the Nordic Seas.

The salinity in the Nordic Seas increased in the upper layers since 2000 (Figure 40). Also in the basin water of the Sogndalsfjord an increase in salinity can be detected since 2000. Only in the basin water of the Barsnesfjord the salinity values dropped in the last period from 2000-2013 (Figure 47).
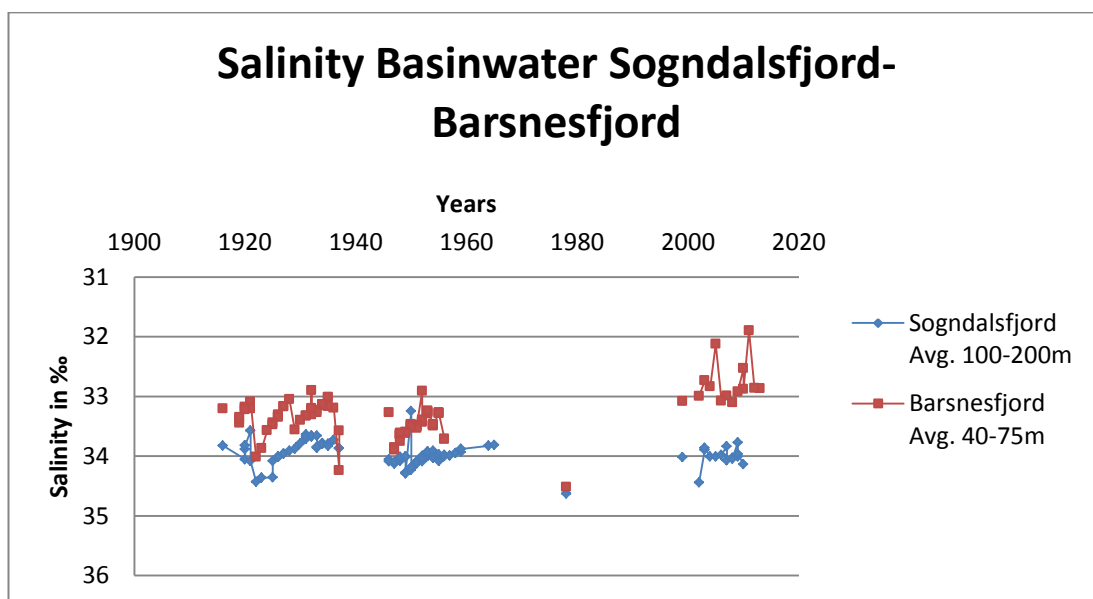

Figure 47: Comparison of salinity in ‰ in the Basin waters of the Sogndalsfjord and the Barsnesfjord. The Sogndalsfjord is represented by the blue line, showing the depths 100, 150 and 200 m. The Barsnesfjord is represented by the red line and shows the depths 40, 50, 60, 75 m.

This decrease can therefore not be explained by the influence of the Sogndalsfjord or the Nordic Seas. Table 5 shows a decrease in salinity in all depths. The table depicts the average salinity of the three main periods of measurement. The decrease from the first to the last period is laying between 0.5‰ and 0.62‰ in the depths of 20-75 m.

Table 5: Average salinity values of the three main periods. The first column depicts the depths in meter from 0 to 75m. The second column shows the average salinity in the first period from 1916-1937 from every depth. The third column depicts the second period from 1946-1956 and the forth column shows the third period from 2002-2013. The last column represents the decrease in salinity from the first to the third period in ‰.

Depths	1.) 1916-1937	2). 1946-1956	3.) 2002-2013	1. and 3. period
in m	Salinity in ‰	Salinity in ‰	Salinity in ‰	Decrease in ‰
0	7,29	5,54	0,44	6,85
5	22,27	22,40	19,56	2,71
10	31,00	30,70	29,45	1,56
20	32,87	33,11	32,38	0,50
30	33,13	33,38	32,64	0,49
40	33,24	33,41	32,68	0,57
50	33,32	33,47	32,74	0,58
60	33,33	33,53	32,79	0,54
75	33,37	33,58	32,76	0,62

The fall in salinity could be due to the increasing precipitation in the area, caused by the positive NAO winter index trend which occurred since around 1980 (Figure 41). This positive NAO winter index leads to south-westerly winds, which then result in more and stronger winter storms reaching Norway and thus bringing more precipitation.

Another factor for lower salinity in the basin water in the Barsnesfjord is the freshwater outflow in wintertime due to the hydroelectric power production using dammed water.

6. Conclusion

This Bachelor Thesis dealt with finding possible explanations for the increasing water temperatures and decreasing oxygen concentrations as well as decreasing salinities within the water column of the Barsnesfjord during the last 100 years:

(1) Throughout the whole water column of the Barsnesfjord, except in the 0 m layer, the water temperatures increased during the last 100 years. This rise happened between 1956 and 2000.

(2) The oxygen concentrations of the Barsnesfjord decreased throughout the entire water column during the last 100 years. During the last decade even critical oxygen levels below 2 mg/l reached as shallow as 30 m.

(3) Oxygen solubility is strongly dependent on the water temperature and decreases at higher temperatures, since the water cannot hold enough oxygen and respiration increases with increasing temperature. Thus changes in the temperature of a water body implicate automatically changes in the oxygen concentrations.

(4) The observed temperature and oxygen variations of the Barsnesfjord occur at the same time as the temperature and oxygen variations of the Sogndalsfjord and the Nordic Seas. It is therefore suggested, that these water variations are related. Changes occurring in the Open Sea can also be seen in both the Sogndalsfjord and the Barsnesfjord.

(5) The salinity values of the Barsnesfjord have decreased during the last 100 years throughout the whole water column.

(6) The Great Salinity Anomaly and the increasing water temperatures of the Nordic Seas correspond to the atmospheric variations of the NAO winter index. The salinity variations of the surface water masses of the Barsnesfjord are also connected to the NAO winter index, since it influences the precipitation pattern.

(7) It can be concluded that the NAO winter index influences the water temperatures and oxygen concentrations of the Nordic Seas, and thereby indirectly influences the water temperatures and oxygen concentrations of the Sogndalsfjord and the Barsnesfjord through water exchange processes. Since these changes are occurring due to natural forces, it is hard to take actions against the increasing water temperatures and the decreasing oxygen concentrations.

(8) It can be tried to reduce the human affected forces that lower oxygen concentrations, as the adding sewage to the fjord. Local forces that changed the inflow regime and the density, like the building of the hydroelectric power plants and the building of the Loftesnes Bridge, cannot be withdrawn. The Barsnesfjord is very sensitive to effects that change the inflowing possibility. Thus it would be recommendable that the sill between Sogndalsfjord and Barsnesfjord should not be narrowed any further, due to the building of a new bridge. Other than that it is hard to make changes that trace back to uncontrollable natural forces.

References

Aa, A. R. 1982: lce movements and deglaciation in the area between Sogndal and Jostedalsbreen, western Norway. Norsk Geologisk Tidsskrift 62, pp. 179-190

American Meteorological Society (2006): Oceans vertical structure background. Online access at: http://oceanmotion.org/html/background/ocean-vertical-structure.htm

Bader, S. & Kunz, P. (2000): *Climate Risks – The Challenge for Alpine Regions*. Vdf Hochschulverlag AG, Zürich, Schweiz, p. 32

Belkin, I.M.; Levitusa, S.; Antonova, J. & Malmberg, S.-A. (1998): *"Great Salinity Anomalies" in the North Atlantic*. In: Progress in Oceanography 41, pp. 1-68. Online access at: http://ac.els-cdn.com/S0079661198000159/1-s2.0-S0079661198000159-main.pdf?_tid=80cdbcef3fcb32fe3b255c5518fa7e30&acdnat=1334137055_f80173f85afe21062d997706f5664e05

Blindheim, J. & Rey, F. (2004): *Water-mass formation and distribution in the Nordic Seas during the 1990s*. In: ICES Journal of Marine Science, 61, pp. 846-863. Online access at: http://icesjms.oxfordjournals.org/content/61/5/846.full.pdf+html

Blindheim, J. & Østerhus, S. (2005): *The Nordic Seas – main oceanographic features.* In: H. Drange, T. Dokken, T. Furevik, R. Gerdes, W. Berger (eds.): The Nordic Seas: An Integrated Perspective. In: American Geophysical Union, Washington DC, AGU Monograph 158, pp. 11-37. Online access at: http://books.google.no/books?id=gXC09wPIL5MC&printsec=frontcover&hl=no&source=gbs_ge_summary_r&cad=0#v=onepage&q&f=false

Cicero (2014): *Weather ship Polarfront: The flagship of climate research*. Online access at: http://www.cicero.uio.no/fulltext/index_e.aspx?id=6340

Climate Data Guide (2014): *Hurrell North Atlantic Oscillation (NAO) Index (station-based)*. Online access at: https://climatedataguide.ucar.edu/climate-data/hurrell-north-atlantic-oscillation-nao-index-station-based

Cottier, F.R. (2010): *Arctic fjords: a review of the oceanographic environment and dominant physical processes*. In: Geological Society, London, Special Publications 2010; pp. 35-50

Department of Oceanography (2005): *Measurement of Temperature and Salinity with Depth*. Online access at: http://oceanworld.tamu.edu/resources/ocng_textbook/chapter06/chapter06_09.htm

Dickson, B. & Østerhus, S. (2007): *One hundred years in the Norwegian Sea.* Norsk Geografisk Tidsskrift - Norwegian Journal of Geography, 61:2, pp. 56-75. Online access at: http://www.tandfonline.com/doi/pdf/10.1080/00291950701409256

EuroSites (2014a): *European Ocean Observatory Network*. Online access at: http://www.eurosites.info/stationm.php

EuroSites (2014b): *European Ocean Observatory Network*. Online access at: http://www.eurosites.info/stationm/data.php

EPA (2012): Dissolved oxygen depletion in Lake Erie. In: United States Environmental Protection Agency – Great Lakes Monitoring. Online access at:

Global Britannica (2014): *Norway Current*. Online access at: http://global.britannica.com/EBchecked/topic/420307/Norway-Current

Helmond, I. (2000): *Oceanographic instrumentation*. Online access at: http://www.es.flinders.edu.au/~mattom/IntroOc/notes/lecture13.html

http://www.es.flinders.edu.au/~mattom/IntroOc/notes/figures/fig13a10.html

Hurrell, J.W. (1995): *Decadal Trends in the North Atlantic Oscillation: Regional Temperatures and Precipitation*. In: Science 269, pp. 676-679. Online access at: http://www.o3d.org/abracco/Atlantic/NAO/hurrell.pdf

Hurrell, J.W., Kushnir, Y., Visbeck, M., Ottersen, G. (2003): An overview of the North Atlantic Oscillation. In: Hurrell, J.W., Kushnir, Y., Ottersen, G., Visbeck, M. (Eds.) The North Atlantic Oscillation, Climatic Significance and Environmental Impact. AGU Geophysical Monograph, vol. 134, pp. 1–35

Hurrell, J.W. & Deser, C. (2009): *North Atlantic climate variability: The role of the North Atlantic Oscillation*. In: Journal of Marine Systems 78 (1), pp. 28-41. Online access at: http://www.sciencedirect.com/science/article/pii/S0924796309000815

NeMo Explorer (2014): *Mid-ocean ridges*. Online access at: http://www.pmel.noaa.gov/eoi/nemo/explorer/concepts/mor.html

NOAA Ocean Service Education (2014): *Currents*. Online access at: http://oceanservice.noaa.gov/education/tutorial_currents/05conveyor2.html

Paetzel, M. & Dale, T. (2010): *Climate proxies for recent fjord sediments in the inner Sognefjord region, western Norway*. In: Geological Society, London, Special Publications 2010; pp. 271-288

Pearson (2014): *Measuring Temperature and Metabolic Rate*. Online access at: http://www.phschool.com/science/biology_place/labbench/lab10/temprate.html

Perillo, G.M.E. (1995): *Geomorphology and Sedimentology of Estuaries*. Elsevier Science, pp. 152- . Online access at: http://books.google.no/books?id=xwKt81JTfp0C&pg=PA152&lpg=PA152&dq=renewal+basin+water+fjord+tidal+forces&source=bl&ots=_lWHrFrZK9&sig=Qk8cvfHxI8Ht_UYKfiwoFiO6uQU&hl=de&sa=X&ei=9LxKU_-_GsXLtAb56YDwCw&ved=0CC0Q6AEwAQ#v=onepage&q=renewal%20basin%20water%20fjord%20tidal%20forces&f=false

Red map (2014): *Upwelling and Downwelling in the ocean*. Online access at: http://www.redmap.org.au/article/upwelling-and-downwelling-in-the-ocean/

SAIV/ AS (2014): *CTD/STD - model SD204 (CTD profiler)*. Online access at: http://www.saivas.no/visartikkel.asp?art=2

Science Daily (2014): *Mid-ocean ridge*. Online access at: http://www.sciencedaily.com/articles/m/mid-ocean_ridge.htm

Sea-Bird Electronics, Inc., (2014): Online access at: http://seabird.com/products/spec_sheets/16plusIMdata.htm

Serreze, M.C. & Barry, R.G. (2005): *The Arctic Climate System*. Cambridge University Press, Cambridge, UK, p. 207. Online access at: http://books.google.no/books?id=k46foPS-JsIC&pg=PA204&hl=de&source=gbs_toc_r&cad=4#v=onepage&q&f=false

Skjoldal, H.R. (2004): *The Norwegian Sea Ecosystem*. Tapir Academic Press, Trondheim, pp. 7-97

Skreslet, S. (1986): *The Role of Freshwater Outflow in Coastal Marine Ecosystems*. Springer Verlag, Berlin Heidelberg, p.31

Surlemont, K. (2012): Bachelorthesis: A 100 year warming of the Sogndalsfjord water column (Western Norway); effects and possible reasons. University of Applied Science Bingen

Syvitski, J.P.M.; Burrell, D.C. & Skei; J.M. (1987): *Fjords: Processes & Products*. Springer Verlag, New York, pp. 379

Sætre, R. (2007): *The Norwegian Coastal Current- Oceanography and Climat*e. Tapir Academic Press, Trondheim, pp. 159

Timmermann, A.; Latif, M.; Voss, R. & Grötzner, A. (1998): *Northern hemispheric interdecadal variability: a coupled air-sea mode*. Journal of Climate 11, pp. 1906-1931. Online access at: http://journals.ametsoc.org/doi/pdf/10.1175/1520-0442(1998)011%3C1906%3ANHIVAC%3E2.0.CO%3B2#h4

UNEP/GRID-Arendal (2007): *World ocean thermohaline circulation*. Online access at: http://www.grida.no/graphicslib/detail/world-ocean-thermohaline-circulation_79a9

Visbeck, M. (2014): *North Atlantic Oscillation.* Online access at:
http://www.ldeo.columbia.edu/res/pi/NAO/

Østerhus, S. & Gammelsrød, T., (1999): *The Abyss of the Nordic Seas Is Warming.* In:
American Meteorological Society, Journal of Climate 12, pp. 3297-3304. Online
access at: http://journals.ametsoc.org/doi/pdf/10.1175/1520-
0442(1999)012%3C3297%3ATAOTNS%3E2.0.CO%3B2

Appendix A
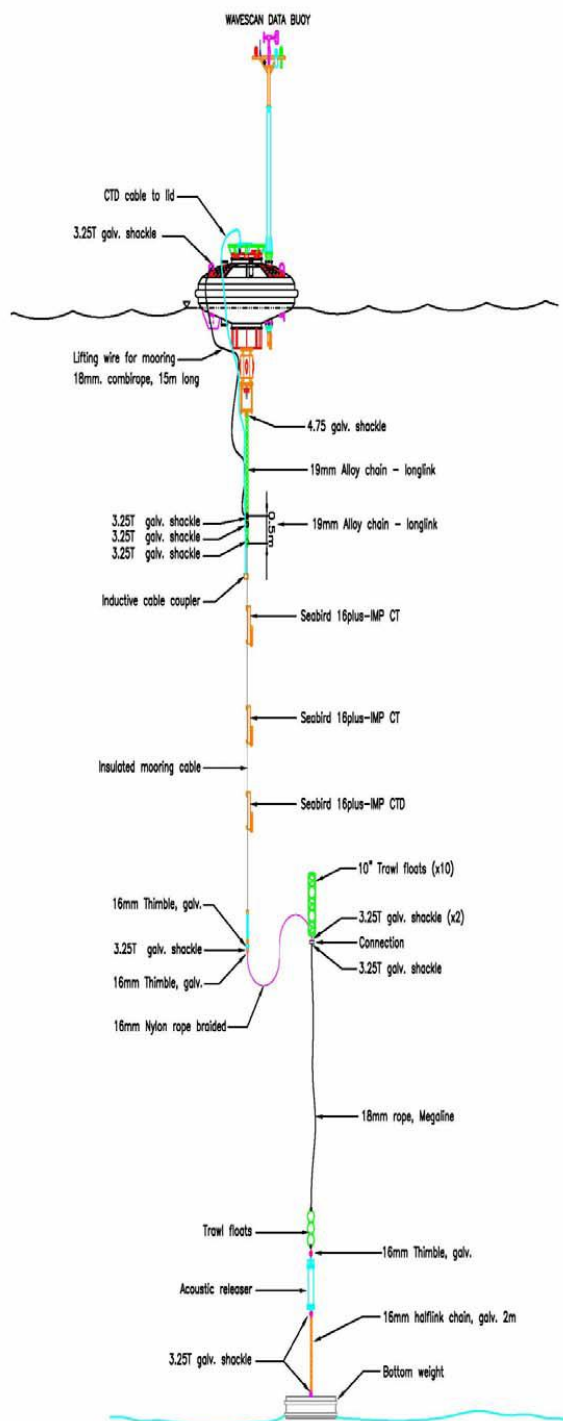
Appendix A: Mooring design for "Station M" (http://www.eurosites.info/stationm/data.php, 2014)

Appendix B

CD includes:

-Summary of The Barsnesfjord data

-Summary of The Sogndalsfjord data

-Folder: Barsnesfjord raw data

-Bachelorthesis.Kaufmann.pdf